

# Evaluation of Thermal Maturity in the Low Maturity Devonian Shales of the Northern Appalachian Basin\*

Robert T. Ryder<sup>1</sup>, Paul C. Hackley<sup>1</sup>, Hossein Alimi<sup>2</sup>, and Michael H. Trippi<sup>1</sup>

Search and Discovery Article #10477 (2013)\*\*

Posted March 31, 2013

\*Manuscript received and accepted January 9, 2013. First presented at AAPG Eastern Section Meeting, 25-29 September 2010, Kalamazoo, Michigan.

\*\*AAPG©2012 Serial rights given by author. For all other rights contact author directly.

<sup>1</sup>U.S. Geological Survey, MS 956 National Center, 12201 Sunrise Valley Drive, Reston, VA 20192 ([phackley@usgs.gov](mailto:phackley@usgs.gov))

<sup>2</sup>Weatherford Laboratories, Geochemical Services Division, 143 Vision Park Blvd., Shenandoah, TX 77384

## Abstract

Thermal maturity of Devonian shales in the northern Appalachian Basin was determined on dip-oriented cross-sections by evaluation of multiple parameters, including gas chromatography (GC) spectra of bitumen extracts, organic matter type, spectral fluorescence of *Tasmanites* algae, and hydrogen index (HI) values. These parameters were compared to Devonian shale thermal maturity determined by random vitrinite reflectance ( $R_o$ ) and the thermal maturity of overlying Pennsylvanian coal determined by maximum vitrinite reflectance ( $R_{o(max)}$ ). Devonian shale  $R_o$  values commonly are lower than overlying Pennsylvanian coal  $R_{o(max)}$  values; this suggests a thermal maturity inversion and the possibility of vitrinite reflectance suppression in shale. However, application of a suppression correction factor to shale  $R_o$  values gave inconsistent results, and this technique was discounted for our data set. Instead, we propose that low  $R_o$  values in low maturity Devonian shale result from inclusion of solid bitumen reflectance measurements in vitrinite reflectance histograms. In contrast, GC spectra, organic matter type, spectral fluorescence of *Tasmanites* algae, and HI values all suggest that shale thermal maturity is higher than determined via  $R_o$  and is more consistent with  $R_{o(max)}$  of overlying coals, especially in the northern part of the study area. Evaluation of HI values may be a better approach to determination of thermal maturity in low maturity shales because it is the least labor intensive and least expensive test; however, this parameter needs to be calibrated vs. atomic H/C ratios. Despite that our new data suggest Devonian shale is higher maturity in the northern part of the study area than previously documented by vitrinite reflectance, it does not explain the presence of dominantly dry thermogenic gas associated with Type II kerogen-bearing oil-prone source rocks.

## Introduction

The regional Devonian shale-gas accumulation in the Appalachian Basin primarily consists of the Middle Devonian Marcellus Shale producing trend in Pennsylvania, West Virginia, and New York, and the overlapping Upper Devonian Ohio Shale producing trend in southern and western West Virginia, eastern Kentucky, eastern Ohio, and southwestern Virginia ([Figure 1](#)). Overall, the regional Devonian shale-gas accumulation follows the northeast trend of the Appalachian Basin and is approximately 600 miles (mi) long by 100-200 mi wide. Thermal maturity of the regional Devonian shale-gas accumulation is characterized by vitrinite reflectance ( $R_o$ ) values that range from about 0.5 % at the

western margin of the gas accumulation to greater than 3.5 % at the eastern margin of the accumulation.  $R_o$  isograds are based on reflectance values of dispersed vitrinite measured from well cuttings and core updated from Repetski et al. (2008).

In contrast, the  $R_{o(max)}$  0.6 % Pennsylvanian coal isograd (based on maximum reflectance of *in situ* vitrinite in coal beds) (Ruppert et al., 2010) (Figure 2) is up to 50 mi west of the Devonian shale  $R_o$  0.5 % isograd, thus indicating that Pennsylvanian coal beds commonly have a higher thermal maturity than Devonian shale that underlies the coal by 1500 to 2000 ft. This apparent “inverted” thermal maturity profile is most pronounced in east-central Ohio as recognized by Rowan et al. (2004) from regional burial history models. A similar “thermal maturity inversion” between Devonian shale and overlying Pennsylvanian coal beds was noted in the Illinois Basin (Barrows and Cluff, 1984; Nuccio and Hatch, 1996). The “inverted” thermal maturity profile recognized in east-central Ohio is replaced farther eastward by a “normal” thermal maturity profile (that is, the Devonian shale  $R_o$  values are about equal to or greater than the Pennsylvanian coal bed  $R_{o(max)}$  values) in eastern Kentucky, southeastern Ohio, western Pennsylvania, and West Virginia (Figure 2). Assuming Pennsylvanian coal  $R_{o(max)}$  values (based on *in situ* vitrinite) to be accurate, one must conclude that Devonian shale  $R_o$  values in east-central Ohio are anomalously low. Moreover, areas with “inverted” thermal maturity profiles (such as east-central Ohio) are confined to immature to low maturity black shale ( $R_o$  values =0.5 %), whereas areas with “normal” thermal maturity profiles (such as southeastern Ohio, western Pennsylvania, and West Virginia) are confined to moderate maturity black shale ( $R_o$  values =1.0 %). Dispersed vitrinite  $R_o$  values may be anomalously low in thermally immature to low maturity organic-rich Devonian shales because of vitrinite suppression, a condition in which the normal kinetics of vitrinite thermal maturation were impacted by a variety of syn-depositional and post-burial processes. Such conditions may include bitumen impregnation, host rock lithology, overpressure, variations in vitrinite precursor material, and incorporation of organic sulfur (Hutton and Cook, 1980; Price and Barker, 1985; McTavish, 1998; Carr, 2000; Barker et al., 2007, among others). Determining if vitrinite reflectance is suppressed in the low maturity shales may have important implications for defining the updip limit of thermogenic gas in the Appalachian Basin.

This investigation has two major objectives: 1) define the western limit of thermogenic Devonian shale-gas in the Appalachian Basin and 2) assess three largely independent properties of Devonian black shale in the Appalachian Basin that may substitute as thermal maturity indicators in place of  $R_o$  data. Assessed properties are as follows: 1. gas chromatographic (GC) spectra of bitumen extracts, 2. maceral types and spectral fluorescence of *Tasmanites* algae, and 3. Rock Eval hydrogen index (HI) values. Each of these properties was evaluated along four dip-oriented transects where  $R_o$  values range from =0.5 to 2.0 % (Figure 3). The four transects (designated A-D) are 160 to 225 mi long, consist of 7 or 8 wells having one or more samples, and extend from Ohio eastward to Pennsylvania, West Virginia, Kentucky, or Virginia. A fifth, much shorter transect (A Lake Erie Shoreline) also was used. The structure and stratigraphy of the transects were constructed specifically for this study using geophysical wireline logs, lithologic logs, geologic maps, and digital elevation models. Correlations in several drill holes relied on previous publications (e.g., Majchszak, 1980; Ryder et al., 2008). Data collected and analyzed on each transect are compiled in Tables 1, 2, 3, and 4.

## Geochemical Character of Devonian Shale

### Total organic carbon (TOC) in weight percent

A histogram of total organic carbon (TOC) values in wt.% (determined by Leco Carbon Analyzer at Weatherford Laboratories) for Devonian shales (n=166) from the subsurface of the Appalachian Basin of Kentucky, New York, Ohio, Pennsylvania, and West Virginia is shown in [Figure 4](#). The TOC distribution ranges from about 0.2 to 15.6 wt.%, and 83 % of the samples contain between 1.0 and 8.2 wt.% TOC. Moreover, the TOC distribution is trimodal with peaks at about 1.4 to 2.2 wt.% (mainly Marcellus Shale from New York, Pennsylvania, and West Virginia, and Rhinestreet Shale from West Virginia), 4.4 to 5.6 wt.% (mainly Marcellus Shale from Pennsylvania and Ohio Shale from Kentucky and Ohio), and 6.0 to 6.8 wt.% (mainly Ohio Shale from Kentucky and Ohio and Marcellus Shale from Ohio and New York). Low TOC (0.2-2.2 wt.%) Devonian shales mainly are Marcellus Shale from West Virginia and Pennsylvania and Rhinestreet Shale from West Virginia. The lower TOC values in this group of samples may be related to the original depositional setting or because of higher thermal maturity.

### Kerogen type

A modified Van Krevelen plot of Devonian shales (n=166) from the subsurface of the Appalachian Basin of Kentucky, New York, Ohio, Pennsylvania, and West Virginia is shown in [Figure 5](#) [determined by Rock-Eval II pyrolysis, e.g., Espitalié et al. (1977) at Weatherford Laboratories]. The large number of samples with hydrogen index (HI) values between 200 and 550 and oxygen index (OI) values between 5 and 15 suggests that the Devonian shale samples are characterized by type II kerogen. Marine origin of the Devonian shale as suggested by the predominance of type II kerogen is consistent with the presence of abundant to common *Tasmanites* (a marine alga) and local conodonts, linguloid brachiopods, and *Tentaculites*. The large number of samples on the Van Krevelen plot with HI values between 0 and 100 and OI values between 5 and 30 most likely represent original type II kerogen converted to type IV kerogen (inert solid bitumen) by thermal degradation.

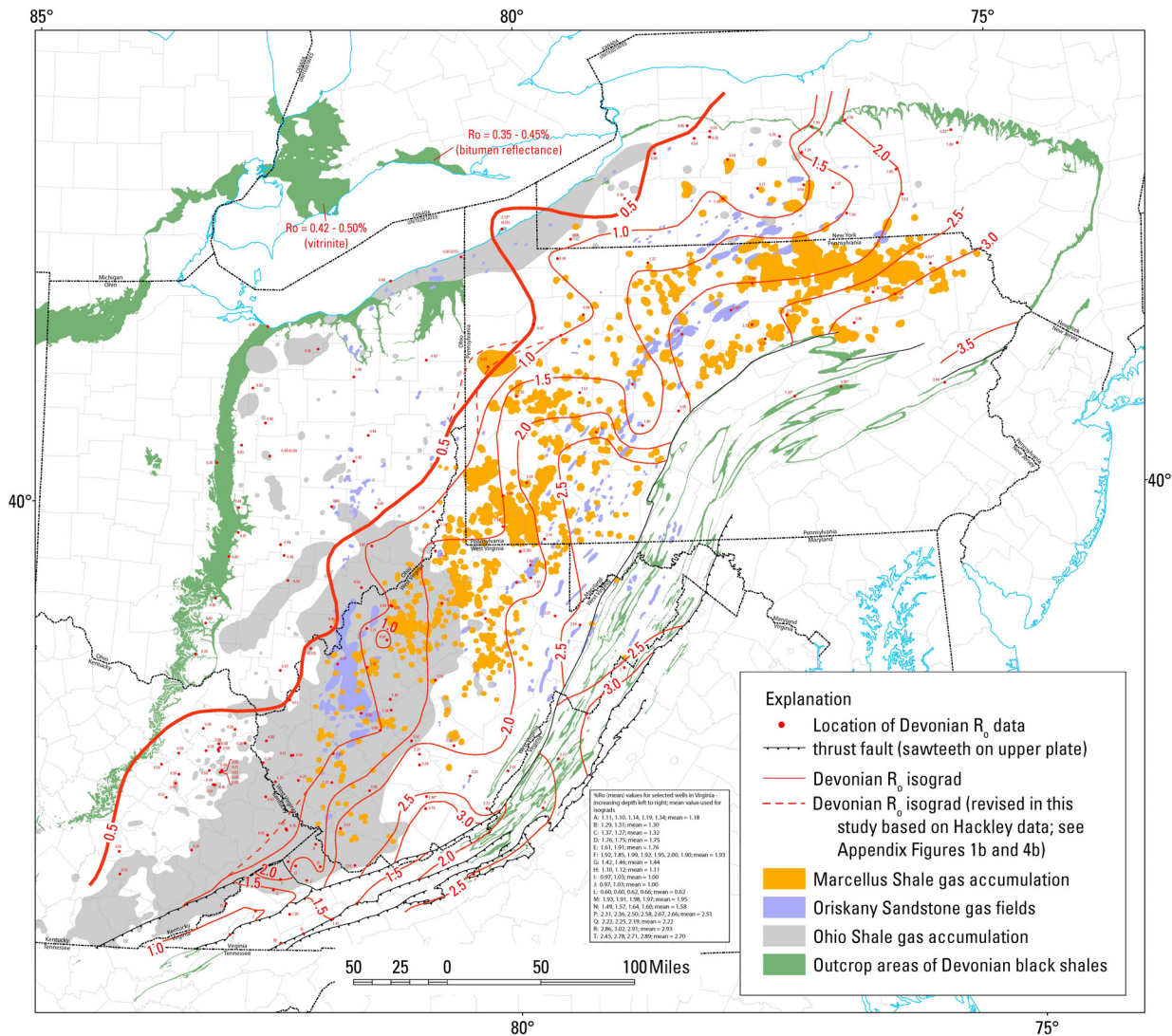


Figure 1

Figure 1. Index map of the Appalachian Basin showing Devonian shale outcrops, shale gas accumulations, and Devonian shale  $R_0$  isograds. Updated from Repetski et al. (2008). Devonian shale  $R_0$  values from Ontario, Canada, from Obermajer et al. (1997). The 0.5% Devonian shale  $R_0$  isograd is shown in bold to emphasize proximity to the onset of hydrocarbon generation.

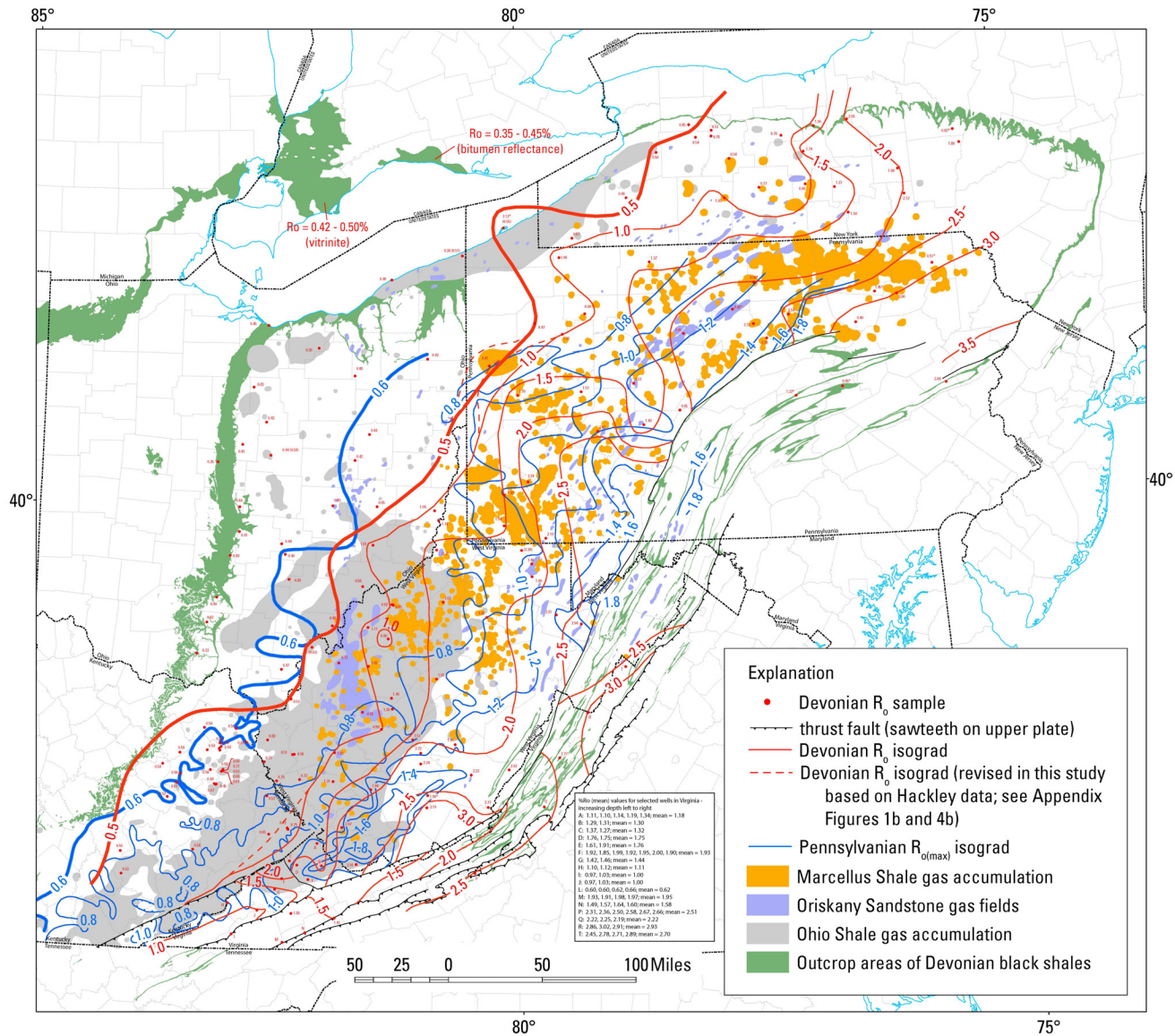


Figure 2

Figure 2. Index map of the Appalachian Basin showing Pennsylvania coal  $R_{o(max)}$  isograds from Ruppert et al. (2010).

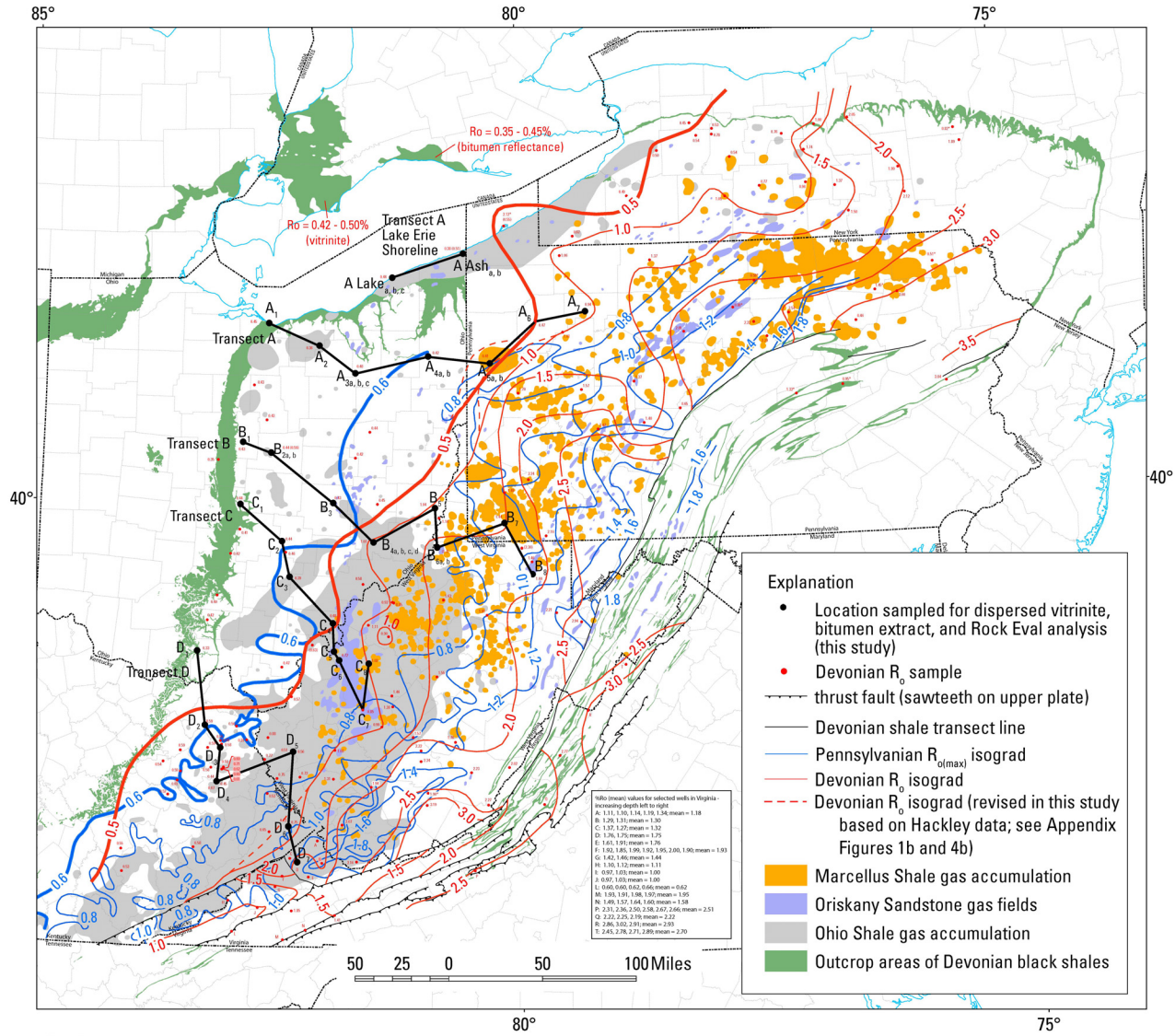
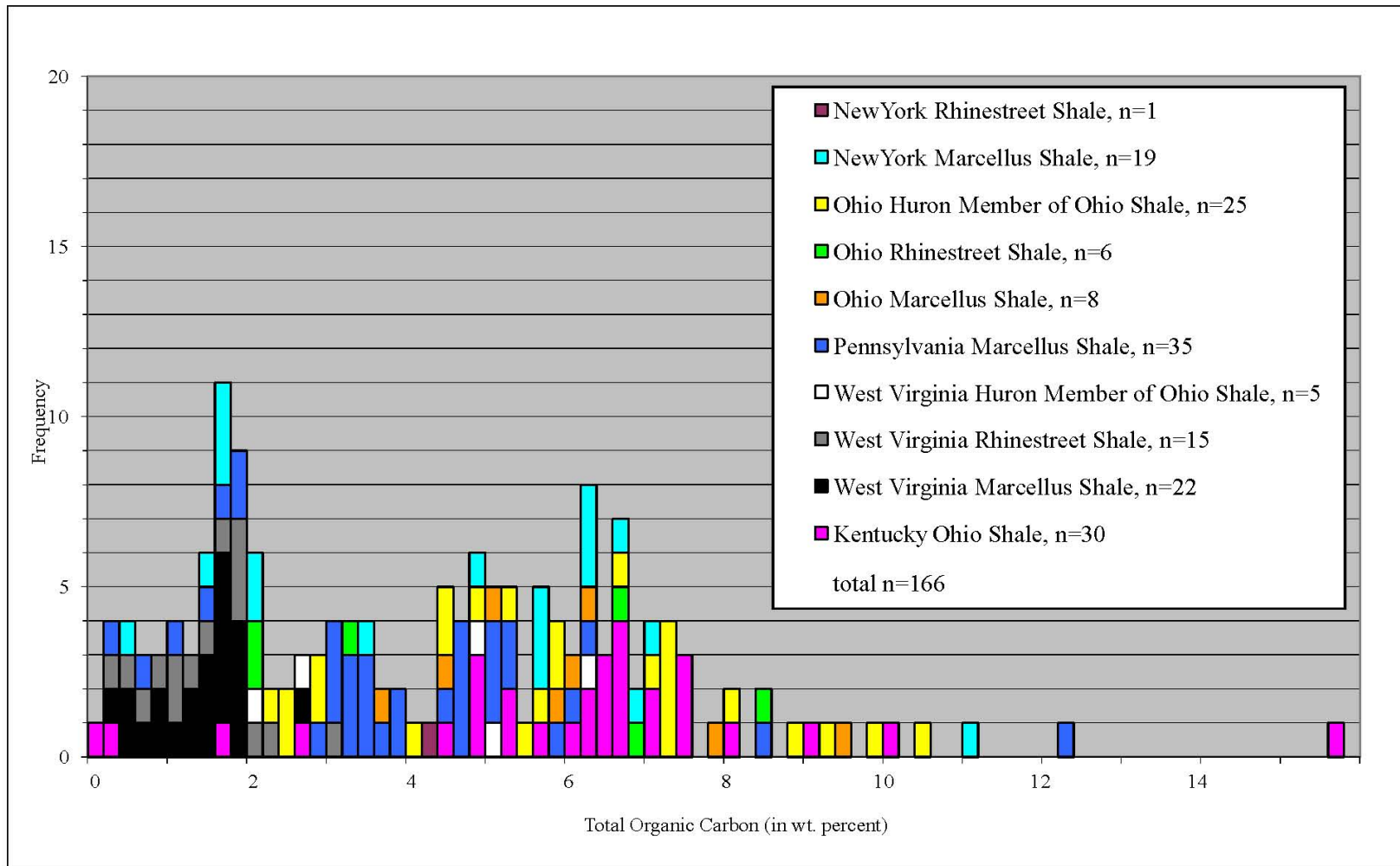


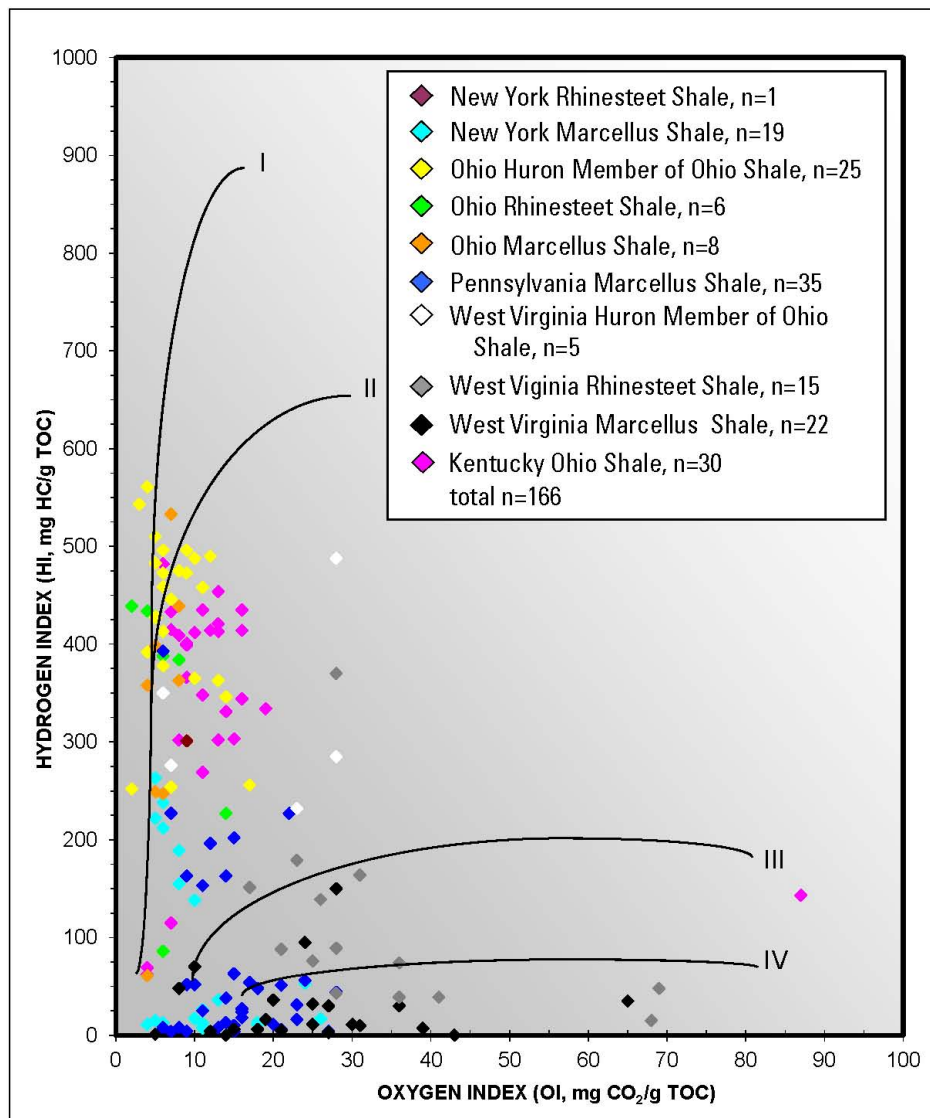
Figure 3

Figure 3. Index map of the Appalachian Basin showing dip-oriented transects A-D and transect A Lake Erie Shoreline used in this study.



**Figure 4**

Figure 4. Histogram showing the distribution of total organic carbon (TOC) in wt.% for Devonian shale samples. Updated from Repetski et al. (2008).



**Figure 5**

Figure 5. Modified Van Krevelen plot (hydrogen index vs. oxygen index) showing kerogen types for Devonian shale samples. Updated from Repetski et al. (2008).

## Distribution of Vitrinite Reflectance ( $R_o$ ) Values along the Transects

### Methodology

The stratigraphy and structure of Middle and Upper Devonian black shales (Marcellus Shale, Rhinestreet Shale, Huron Member of the Ohio Shale, Cleveland Member of the Ohio Shale), Lower Mississippian black shale (Sunbury Shale), and overlying Mississippian and Pennsylvanian strata along transects A-D and A Lake Erie Shoreline are shown in [Figures 6, 7, 8, and 9](#). Also included are the stratigraphic positions of collected samples and results of vitrinite reflectance ( $R_o$ ) measurements. In order to record the maximum  $R_o$  value of the Devonian black shale sequence at each point on the transects, the oldest available black shale unit was collected from each drill hole. Therefore, the Marcellus Shale was the preferred unit to be sampled, followed by the Rhinestreet Shale and the lower part of the Huron Member. Samples from all three of these black shale units have comparable depths of burial whereby no unit is separated stratigraphically by more than 800 ft in each well. The Marcellus Shale, Rhinestreet Shale, and lower part of the Huron Member have similar geochemical properties based on similar environments of deposition, mineralogy, and organic facies (Streib, 1981; Zielinski and McIver, 1982).

The  $R_o$  values were derived from whole-rock core and cuttings samples that were ground to 16-20 mesh size, mounted in plastic and/or epoxy pellets, polished, and measured in oil under reflected light (ASTM 2011a,b). Approximately 20 to 50  $R_o$  measurements of dispersed vitrinite random reflectance were made for each sample and the mean value is reported. Most of the analyses were completed by Humble Geochemical Services (HGS, now Weatherford Laboratories) analysts or Paul C. Hackley (USGS, Reston, VA) and reported in [Tables 1, 2, 3, and 4](#). A small number of  $R_o$  analyses were reported by Streib (1981), Zielinski and McIver (1982), and ExLog Brown and Ruth (1988) ([Tables 1, 2, 3, and 4](#)).  $R_o$  analyses by HGS previously were reported in Repetski et al. (2008).

### Transect A

Transect A extends from north-central Ohio to northwestern Pennsylvania and consists of 7 drill holes ([Figure 6](#)). Transect A Lake Erie Shoreline is located in northeastern Ohio and consists of two drill holes. The subsurface distribution of Devonian shale  $R_o$  and Pennsylvanian coal  $R_{o(max)}$  isograds along transect A is shown in [Figure 10](#) based on map view isograds from Repetski et al. (2008) and Ruppert et al. (2010). As indicated by the map view of Devonian shale and Pennsylvanian coal isograd patterns on [Figure 3](#), the Devonian shale  $R_o$  values on [Figure 10](#) are lower than the overlying Pennsylvanian coal  $R_{o(max)}$  values and, therefore, are consistent with the previously introduced term “thermal maturity inversion.” The “thermal maturity inversion” phenomenon is shown by juxtaposition of Pennsylvanian coal 0.6 % and 0.8 % isograds near drill holes A<sub>4</sub> and A<sub>5</sub>, respectively, against Devonian shale  $R_o$  values of 0.48 to 0.42 % in drill holes A<sub>3</sub> and A<sub>4</sub>. “Thermal maturity inversion” also is characterized by juxtaposition of the estimated Pennsylvanian coal 0.9 % isograd (location estimated from [Figure 3](#) with the Devonian shale 0.5 % isograd near drill hole A<sub>6</sub>. The only area that shows a “normal” thermal maturity profile is where the Devonian shale 1.0 % isograd near drill hole A<sub>7</sub> coincides with the estimated 1.0 % Pennsylvanian coal isograd. An alternate location for the 0.5 % Devonian  $R_o$  isograd shown in [Figure 10](#) is based on the 0.96 value of Hackley ([Table 1](#)) in sample A5a.

## Reproducibility and Suppression Correction Factor

Evaluation of  $R_o$  values determined by different operators indicates a moderate to high level of reproducibility for Transects A and A Lake Erie Shoreline (Figure Appendix 1-a). Application of the  $R_o$  suppression correction factor proposed by Lo (1993) ([Figure 11](#)) resulted in moderate changes to the placement of the Devonian shale  $R_o$  isograds shown in [Figure 10](#). However, changes in the locations of  $R_o$  isograds as a result of application of the suppression correction factor showed no consistent regional pattern (Figure Appendix 1-b), and this technique was discounted for our data set. A detailed evaluation of  $R_o$  data reproducibility and the application of the Lo (1993) suppression correction factor for Transects A and A Lake Erie Shoreline are presented in Appendix 1.

### Transect B

The subsurface distribution of Devonian shale  $R_o$  and Pennsylvanian coal  $R_{o(max)}$  isograds along transect B are shown in [Figure 12](#), based on map view isograds from Repetski et al. (2008) and Ruppert et al. (2010). As indicated by the map view of Devonian shale and Pennsylvanian coal isograd patterns, Devonian shale  $R_o$  values are lower than the overlying Pennsylvanian coal  $R_{o(max)}$  values and, therefore, also show a “thermal maturity inversion.” The “thermal-maturity inversion” is characterized by juxtaposition of the Pennsylvanian coal 0.6 % isograd (between drill holes B<sub>3</sub> and B<sub>4</sub>) against Devonian shale  $R_o$  values of 0.38 to 0.44 % in drill hole B<sub>2</sub> and juxtaposition of the Pennsylvanian coal 0.8 % isograd (between drill holes B<sub>6</sub> and B<sub>7</sub>) against the Devonian shale 0.5 % isograd near drill hole B<sub>3</sub>. The only area that shows a “normal” thermal maturity profile is where the Devonian shale 1.0 and 1.5 % isograds between drill holes B<sub>4</sub> and B<sub>6</sub> coincide with the respective 1.0 and 1.5 % Pennsylvanian coal isograds located between B<sub>7</sub> and B<sub>8</sub>, and east of B<sub>8</sub>, respectively. The 1.5 % Devonian  $R_o$  isograd in [Figure 12](#) is based on the 1.71 value of Streib (1981) in sample B6b, rather than the 1.44 value of HGS in sample B7.

## Reproducibility and Suppression Correction Factor

Evaluation of  $R_o$  values determined by different operators indicates a moderate to high level of reproducibility for Transect B (Figure Appendix 2-a). Application of the  $R_o$  suppression correction factor proposed by Lo (1993) resulted in moderate changes to the placement of the Devonian shale  $R_o$  isograds shown in [Figure 12](#). However, changes in the locations of  $R_o$  isograds as a result of application of the suppression correction factor showed no consistent regional pattern (Figure Appendix 2-b), and this technique was discounted for our data set. A detailed evaluation of  $R_o$  data reproducibility and the application of the Lo (1993) suppression correction factor for Transect B are presented in Appendix 2.

### Transect C

The subsurface distribution of Devonian shale  $R_o$  and Pennsylvanian coal  $R_{o(max)}$  isograds along transect C based on map view isograds from Repetski et al. (2008) and Ruppert et al. (2010) is shown in [Figure 13](#) and also indicates a thermal maturity inversion. The thermal maturity inversion is characterized by juxtaposition of the Pennsylvanian coal 0.6 % isograd near drill hole C<sub>2</sub> against the Devonian shale  $R_o$  value of 0.44 % in drill hole C<sub>1</sub> and juxtaposition of the Pennsylvanian coalbed 0.8 % isograd near drill hole C<sub>7</sub> against the Devonian shale  $R_o$  value of 0.48 % value in drill hole C<sub>4</sub>. Another example of the inverted thermal maturity profile occurs where Devonian shale  $R_o$  values of 0.44 % in

drill hole C<sub>2</sub> and 0.39 % in drill hole C<sub>3</sub> are overlain by Pennsylvanian coal R<sub>o(max)</sub> values that range between 0.6 and 0.8 %. The only area that shows a “normal” thermal maturity profile is where the Devonian shale 1.0 % isograd in drill hole C<sub>8</sub> coincides with the 1.0 % Pennsylvanian coal isograd located about 40 mi east of drill hole C<sub>8</sub>.

### **Reproducibility and Suppression Correction Factor**

Evaluation of R<sub>o</sub> values determined by different operators indicates a moderate to high level of reproducibility for Transect C (Figure Appendix 3-a). Application of the R<sub>o</sub> suppression correction factor of Lo (1993) resulted in moderate changes to the placement of the Devonian shale R<sub>o</sub> isograds shown in [Figure 13](#). However, changes in the locations of R<sub>o</sub> isograds showed no consistent regional pattern (Figure Appendix 3-b), and this technique was discounted for our data set. A detailed evaluation of R<sub>o</sub> data reproducibility and the application of the Lo (1993) suppression correction factor for Transect C are presented in Appendix 3.

### **Transect D**

The subsurface distribution of Devonian shale R<sub>o</sub> and Pennsylvanian coal R<sub>o(max)</sub> isograds along transect D based on map view isograds from Repetski et al. (2008) and Ruppert et al. (2010) is shown in [Figure 14](#). In contrast to transects A through C, transect D shows a “normal” thermal maturity profile at each end of the transect and an inverted thermal maturity profile in the central part of the transect. The central zone of “thermal-maturity inversion” is located where the Devonian shale R<sub>o</sub>=0.45 % value (in drill hole D<sub>4</sub>) and the R<sub>o</sub>=0.51 % value (in drill hole D<sub>5</sub>) underlie the 0.6 to 0.8 % Pennsylvanian coal R<sub>o(max)</sub> isograds. The “normal” thermal maturity profile at the western end of the transect is recognized where the Devonian shale 0.5 % isograd between drill holes D<sub>1</sub> and D<sub>2</sub> is closely aligned with the 0.6 % Pennsylvanian coalbed isograd located between drill holes D<sub>2</sub> and D<sub>3</sub>. Also, the Devonian shale R<sub>o</sub> values of 0.58 to 0.59 % in drill holes D<sub>3</sub> and D<sub>2</sub>, respectively, are considered to be part of the “normal” thermal maturity profile at the western end of the transect even though they are slightly lower than the overlying 0.6 % Pennsylvanian coal isograd. The “normal” thermal maturity profile at the eastern end of the transect is recognized where the Devonian shale 1.0 % isograd and the Devonian shale 1.5 % isograd coincide with respective Pennsylvanian coal 1.0 and 1.5 % isograds. The 1.0 and 1.5 Devonian R<sub>o</sub> isograds in [Figure 14](#) are based on the 1.42 value of Hackley ([Table 4](#)) in sample D6 rather than the 0.75 value of HGS.

### **Reproducibility and Suppression Correction Factor**

Evaluation of R<sub>o</sub> values determined by different operators indicates a moderate level of reproducibility for Transect D (Figure Appendix 4-a). Application of the R<sub>o</sub> suppression correction factor (Lo, 1993) resulted in moderate changes to the placement of Devonian shale R<sub>o</sub> isograds shown in [Figure 14](#). However, changes in the locations of R<sub>o</sub> isograds showed no consistent regional pattern (Figure Appendix 4-b), and this technique was discounted for our data set. A detailed evaluation of R<sub>o</sub> data reproducibility and the application of the Lo (1993) suppression correction factor for Transect D are presented in Appendix 4.

## Discussion

The distribution of Devonian shale  $R_o$  and Pennsylvanian coal  $R_{o(max)}$  isograd patterns shown on [Figures 1, 2, and 3](#) imply unrealistic paleogeothermal relationships for Ohio and adjoining parts of Kentucky, Pennsylvania, and West Virginia because they commonly suggest “inverted” thermal maturity profiles. These unrealistic paleogeothermal relationships are further emphasized in the cross-sections along transects A-D where Devonian shale  $R_o$  values commonly are lower than overlying Pennsylvanian coal  $R_{o(max)}$  values and (or) Devonian shale  $R_o$  isograds are offset from Pennsylvanian coal  $R_{o(max)}$  isograds ([Figures 10, 12, 13, and 14](#)). In general, the “inverted” thermal-maturity profiles occur where Devonian shale  $R_o$  values are between about 0.35 and 0.55 % and overlying Pennsylvanian coal  $R_{o(max)}$  values are between about 0.6 and 0.8 %. Where “normal” thermal maturity profiles are present they commonly are at the southeastern ends of the transects where Devonian shale  $R_o$  and Pennsylvanian coal  $R_{o(max)}$  isograds are closely aligned and are equal to or greater than 1.0 %. In a few cases, “normal” thermal maturity profiles are located toward the northwestern ends of the transects where Devonian shale  $R_o$  and Pennsylvanian coal  $R_{o(max)}$  isograds are closely aligned and equal to 0.5 or 0.6 %.

Based on the preceding discussion, the location of the Devonian shale  $R_o$  0.5 % isograd shown on [Figures 1, 2, and 3](#) probably underestimates the western extent of thermally mature Devonian shale with respect to oil and early gas generation. Consequently, the Devonian shale  $R_o$  0.5 % isograd is considered herein to be an unreliable indicator of the western (updip) limit of thermogenic gas and oil generation in the Devonian shale sequence and should be extended at least 30 to 50 mi westward to where it coincides with the Pennsylvanian coal  $R_{o(max)}$  0.6 % isograd. In contrast, Devonian shales with  $R_o$  values =1.00 % values provide a reliable indication of thermal maturation history. An effort to correct suppression of  $R_o$  values (following Lo, 1993) in the immature to marginally mature Devonian shale ( $R_o=0.7$  %) met with mixed results ([Appendices 1, 2, 3, and 4](#)). Although the correction factor successfully shifted the Devonian shale 0.5 % isograd farther westward in several areas ([Figures Appendix 1-b, 2-b](#)), in most cases the correction factor still underestimated Devonian shale  $R_o$  values or, particularly at the northwestern ends of the transects, overestimated Devonian shale  $R_o$  values ([Figure Appendix 3-b](#)) compared to  $R_{o(max)}$  values of nearby Pennsylvanian coals. Thus, vitrinite suppression corrections are considered herein to provide inconsistent and “artificial”  $R_o$  values that should not be incorporated into regional thermal maturity maps of the Devonian black shales in the Appalachian Basin. For similar reasons, Repetski et al. (2008) chose not to contour “corrected” data points (calculated by HGS; see [Tables 1, 2, 3, and 4](#)) on their Devonian shale  $R_o$  map.

We propose that abnormally low  $R_o$  values recorded in these organic-rich, thermally immature to marginally mature Devonian shales may have resulted from measurement of solid bitumen (or vitrinite-like material). Solid bitumen at these lower thermal maturity levels ( $R_o=0.25$  to 0.70 %) may have different kinetic properties than vitrinite and therefore may yield lower reflectance values (Robert, 1988; Jacob, 1989; Landis and Castaño, 1995). The common occurrence of bitumen is not usual in organic-rich shales that are characterized by type II kerogen. Furthermore, Obermajer et al. (1997) previously reported bitumen reflectance values for the Marcellus Shale along the Lake Erie shoreline in Ontario, Canada ([Figure 1](#)). We speculate that bitumen ranges in composition from gilsonite to grahamite ([Figure 15](#)) and was generated and extruded into microfractures in the organic-rich Devonian black shales early in the maturation cycle. Although this speculation is not supported by an abundance of bitumen “fracture fillings” or “microdikes” in core or outcrop samples, these features have been reported locally along transect A (Cliff Minerals, 1979a,b). Also, larger bitumen dikes have been reported in Pennsylvanian strata from southwestern Pennsylvania (Koppe, 1959; Curiale, 1986) and northwestern West Virginia (Merrill, 1904; Simard, 1985), but it is uncertain whether the bitumen was generated from

underlying Devonian black shales or from within Pennsylvanian black shales and coal beds. Once solid bitumen in the Devonian shales reached thermal maturity values of  $R_o=0.7$  to 1.0 %, its molecular structure may have been modified such that kinetic reactions of bitumen approximate the kinetic reactions of vitrinite and become compatible with the Pennsylvanian coal  $R_{o(max)}$  values. Petrographic observation of our samples documented that some void-filling solid bitumens had similar reflectance values to discrete organic fragments interpreted to be vitrinite. Therefore, a mixture of solid bitumen plus vitrinite reflectance measurements or measurements dominantly of bitumen could be expected as the result of a “vitrinite” reflectance determination on a low-maturity Appalachian or Illinois Basin Devonian shale.

Because Devonian shale  $R_o$  values in the 0.30 to 0.70 % range are highly suspect (including the location of the 0.5 % isograd shown on [Figures 1, 2, and 3](#)), they cannot be used to reliably estimate the onset of oil and (or) thermogenic gas. Consequently, alternative measures must be adopted to better document the onset of the oil and (or) accompanying early thermogenic gas window. The remainder of this report is devoted to systematic study of three physical and geochemical characteristics to determine if they can be correlated with the onset of oil and (or) thermogenic gas in Devonian shales of the Appalachian Basin: 1) gas chromatographic (GC) analysis of bitumen extracts, 2) dispersed maceral types and spectral fluorescence of *Tasmanites* algae, and 3) Hydrogen Index (HI) contours.

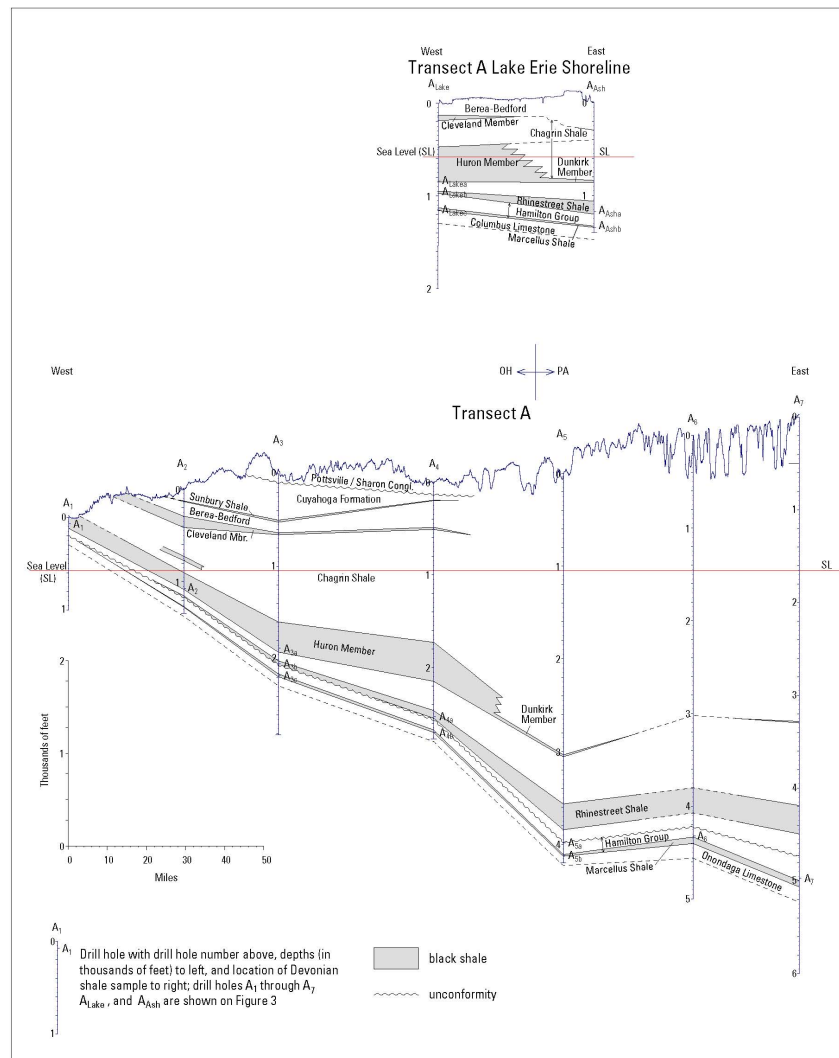
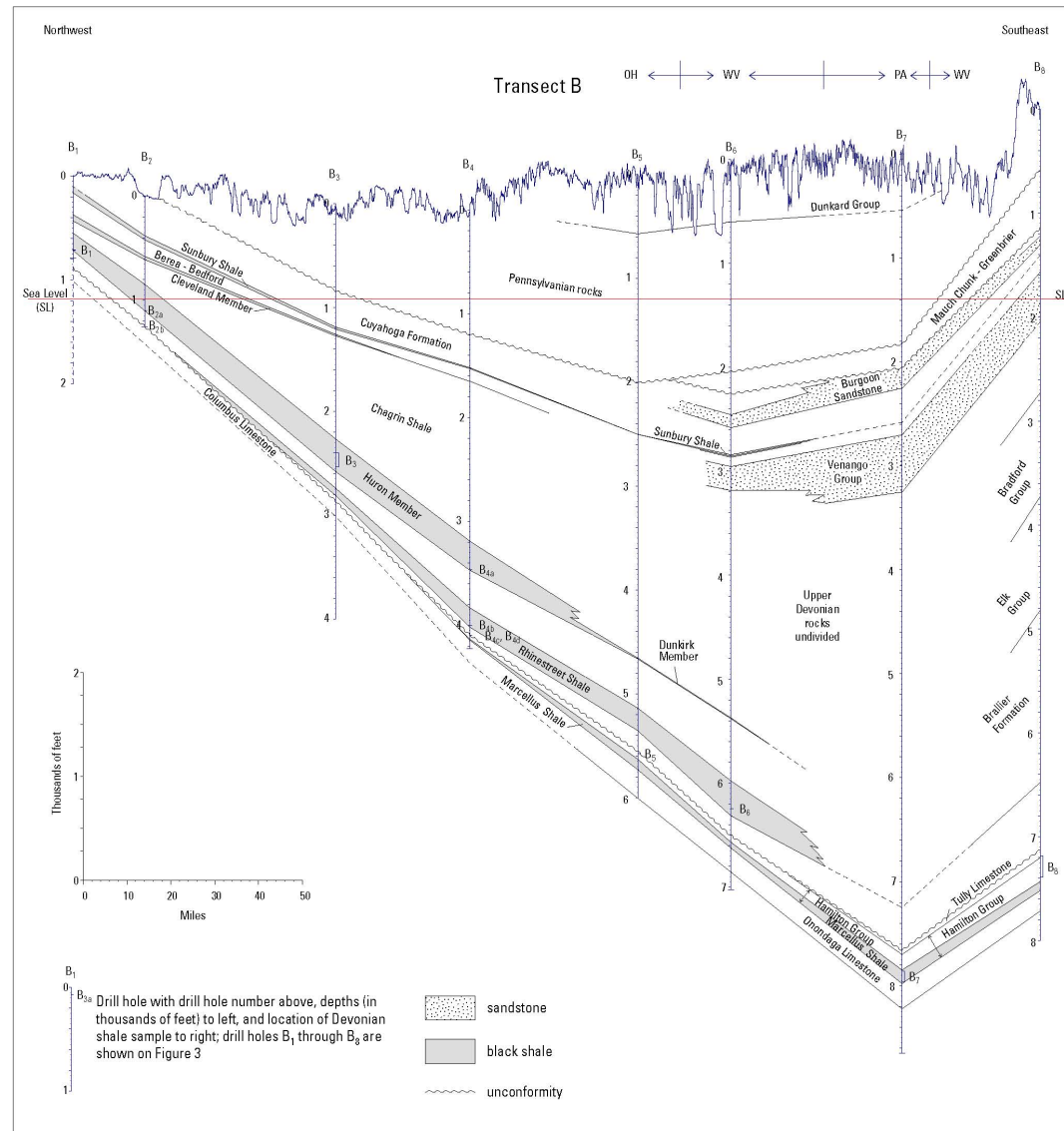


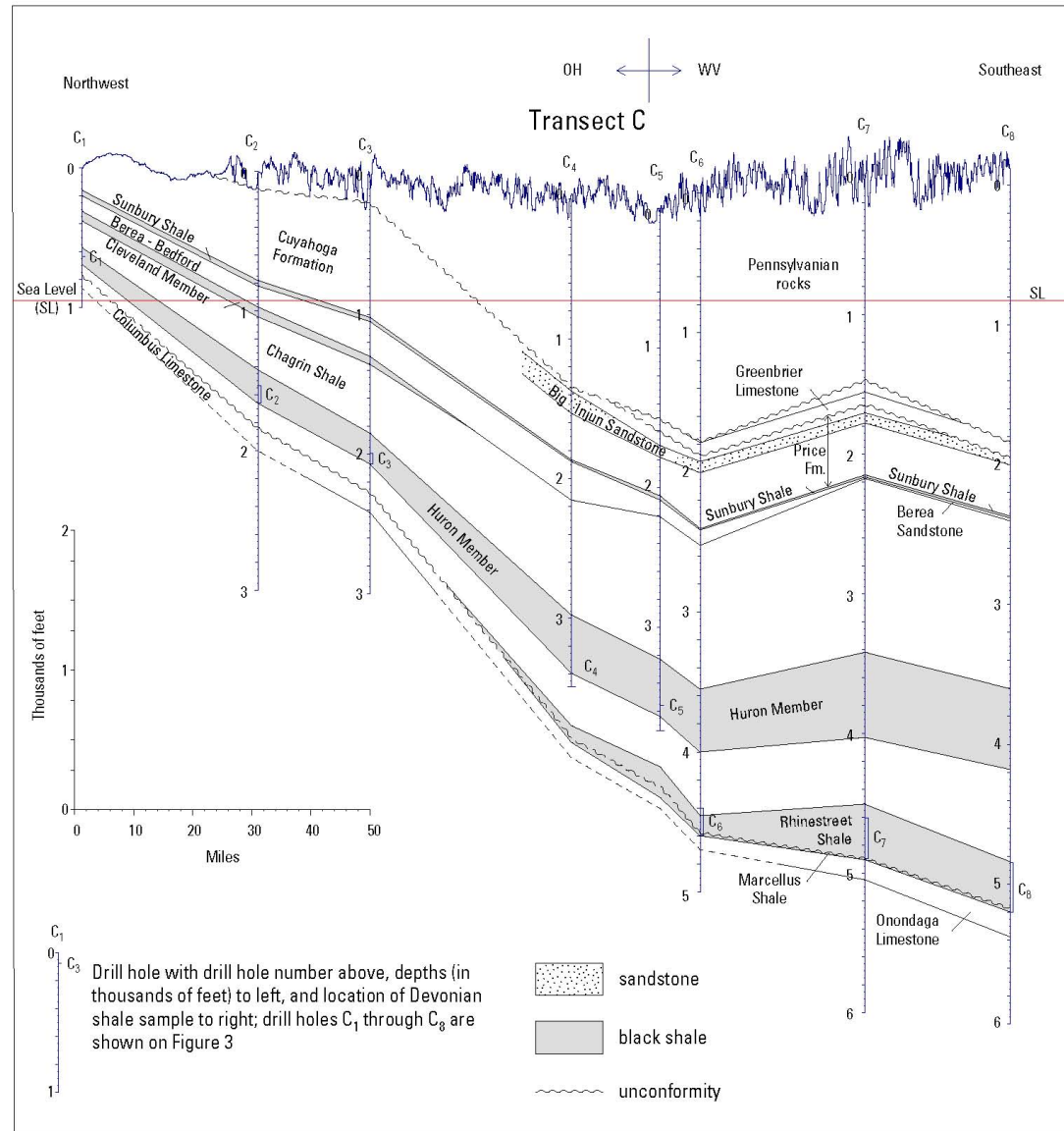
Figure 6

Figure 6. Geologic cross-section along transect A showing the stratigraphy and structure of Devonian black shales and the location of analyzed samples in drill holes A<sub>1</sub>-A<sub>7</sub>. A companion cross-section transect A Lake Erie Shoreline containing drill holes A<sub>Lake</sub> and A<sub>ASH</sub> also is shown. Surface elevation (blue line) in this and other cross-section figures of this article was derived from a digital elevation model evaluated in a geographic information system.



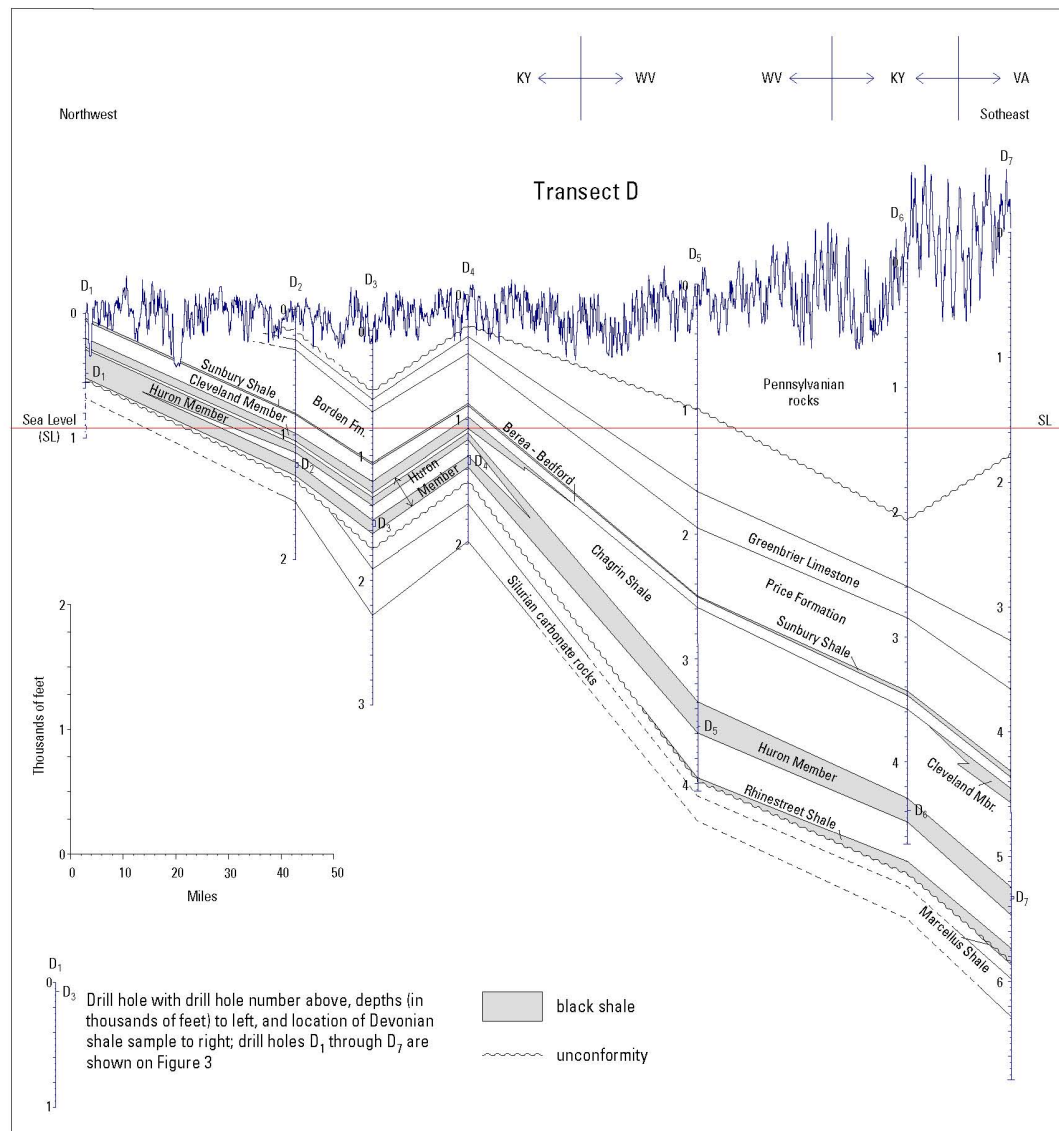
**Figure 7**

Figure 7. Geologic cross-section along transect B showing the stratigraphy and structure of Devonian black shales and the location of analyzed samples in drill holes B<sub>1</sub>-B<sub>8</sub>.



**Figure 8**

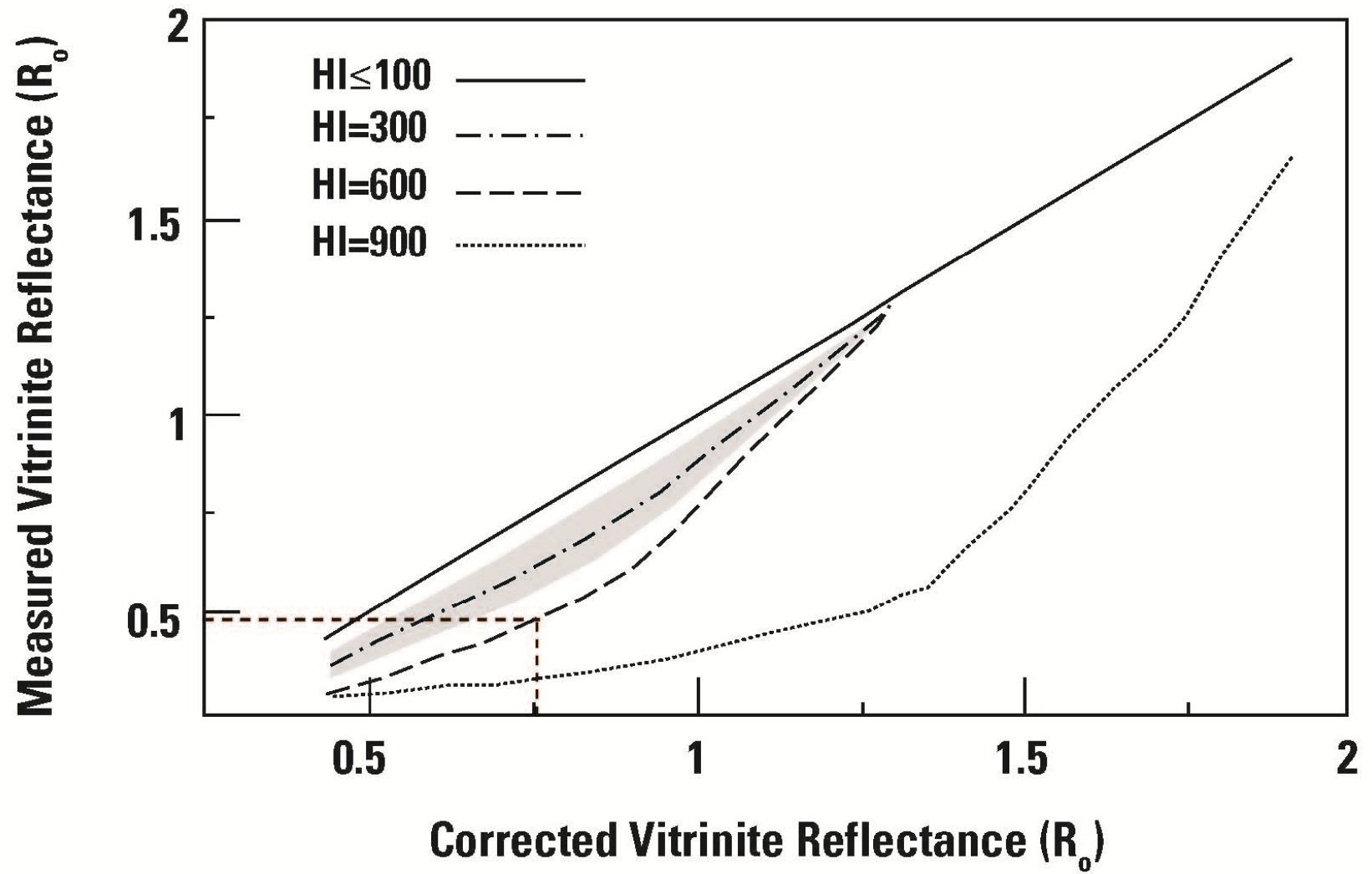
Figure 8. Geologic cross-section along transect C showing the stratigraphy and structure of Devonian black shales and the location of analyzed samples in drill holes C<sub>1</sub>-C<sub>8</sub>.



**Figure 9**

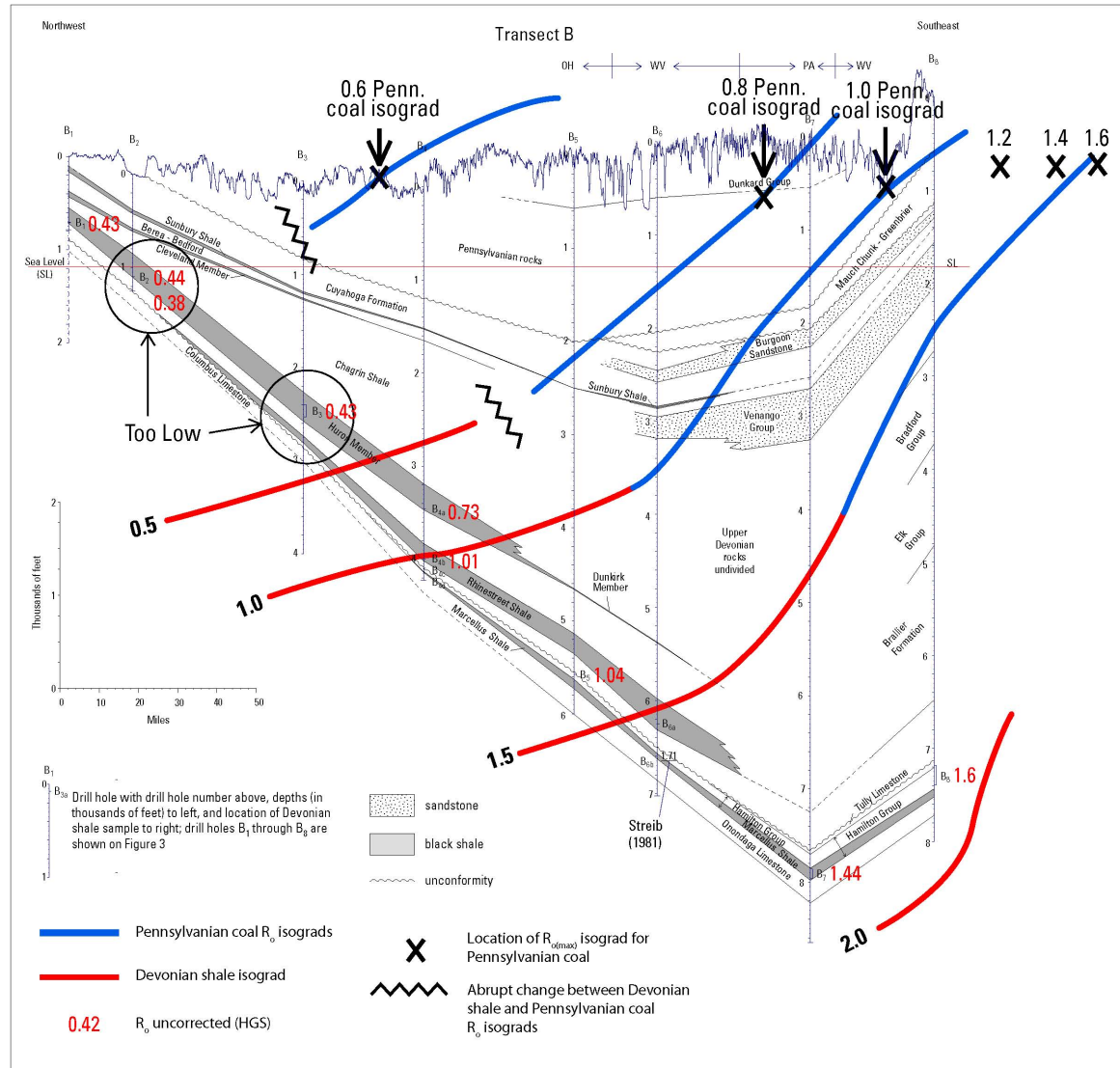
Figure 9. Geologic cross-section along transect D showing the stratigraphy and structure of Devonian black shales and the location of analyzed samples in drill holes D<sub>1</sub>-D<sub>7</sub>.





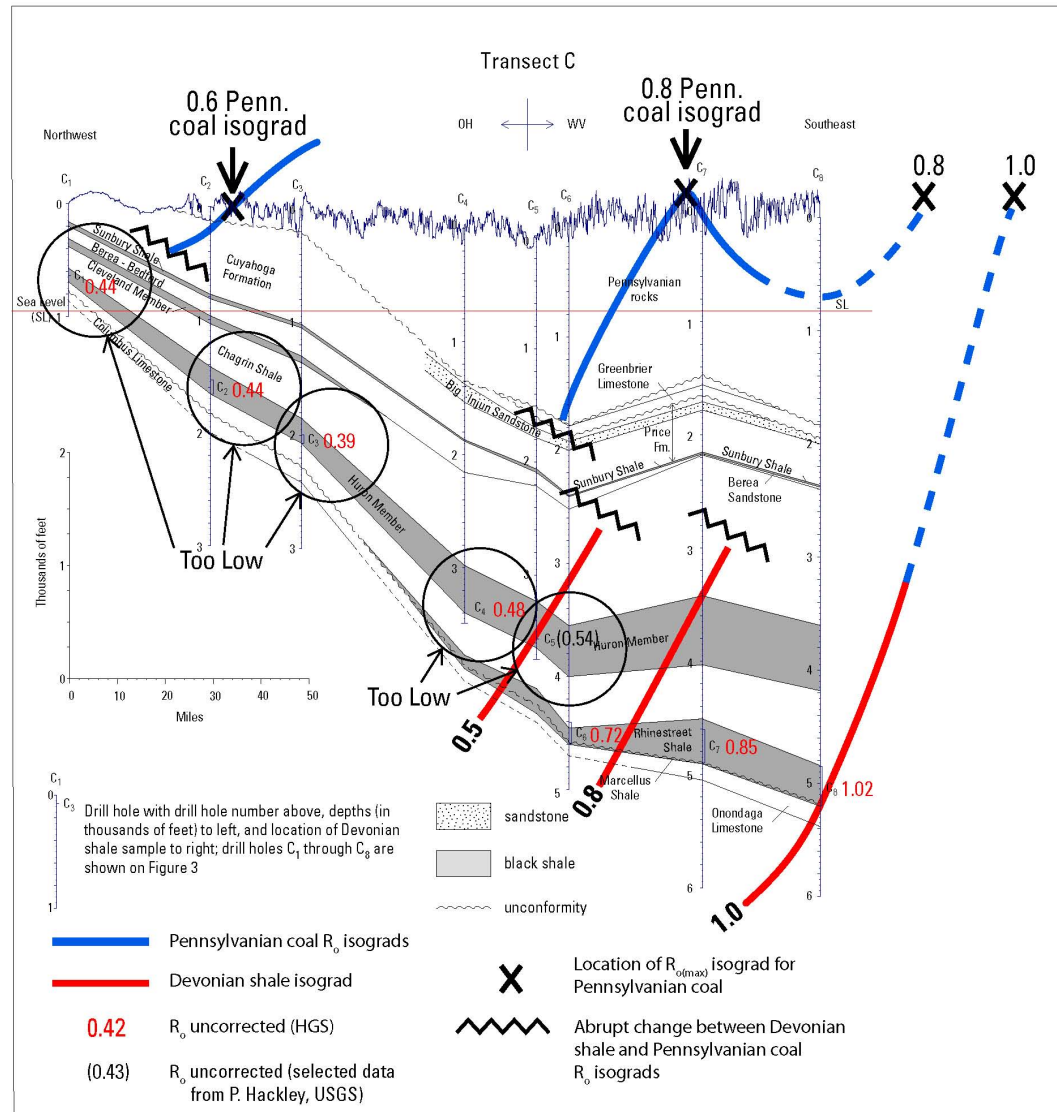
**Figure 11**

Figure 11. Cross plot of measured  $R_o$  vs. corrected  $R_o$  to account for vitrinite reflectance suppression. From Lo (1993).



**Figure 12**

Figure 12. Geologic cross-section along transect B showing the distribution of measured Devonian shale  $R_0$  values and projected subsurface Devonian shale  $R_0$  and Pennsylvanian coal  $R_{0(max)}$  isograds based on map view isograds from Repetski et al. (2008) and Ruppert et al. (2010), respectively. HGS, Humble Geochemical Services.



**Figure 13**

Figure 13. Geologic cross-section along transect C showing the distribution of measured Devonian shale  $R_o$  values and projected subsurface Devonian shale  $R_o$  and Pennsylvania coal  $R_{o(max)}$  isograds based on map view isograds from Repetski et al. (2008) and Ruppert et al. (2010), respectively. HGS, Humble Geochemical Services.

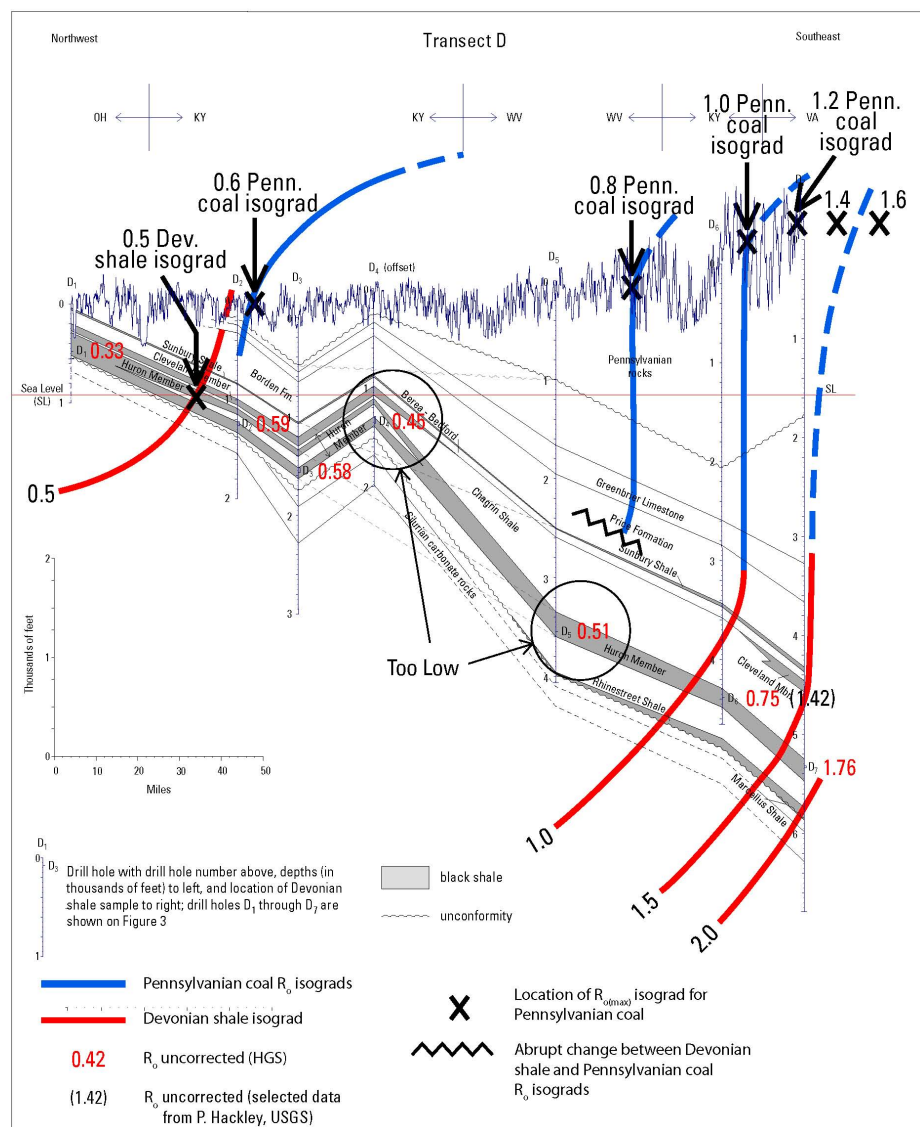
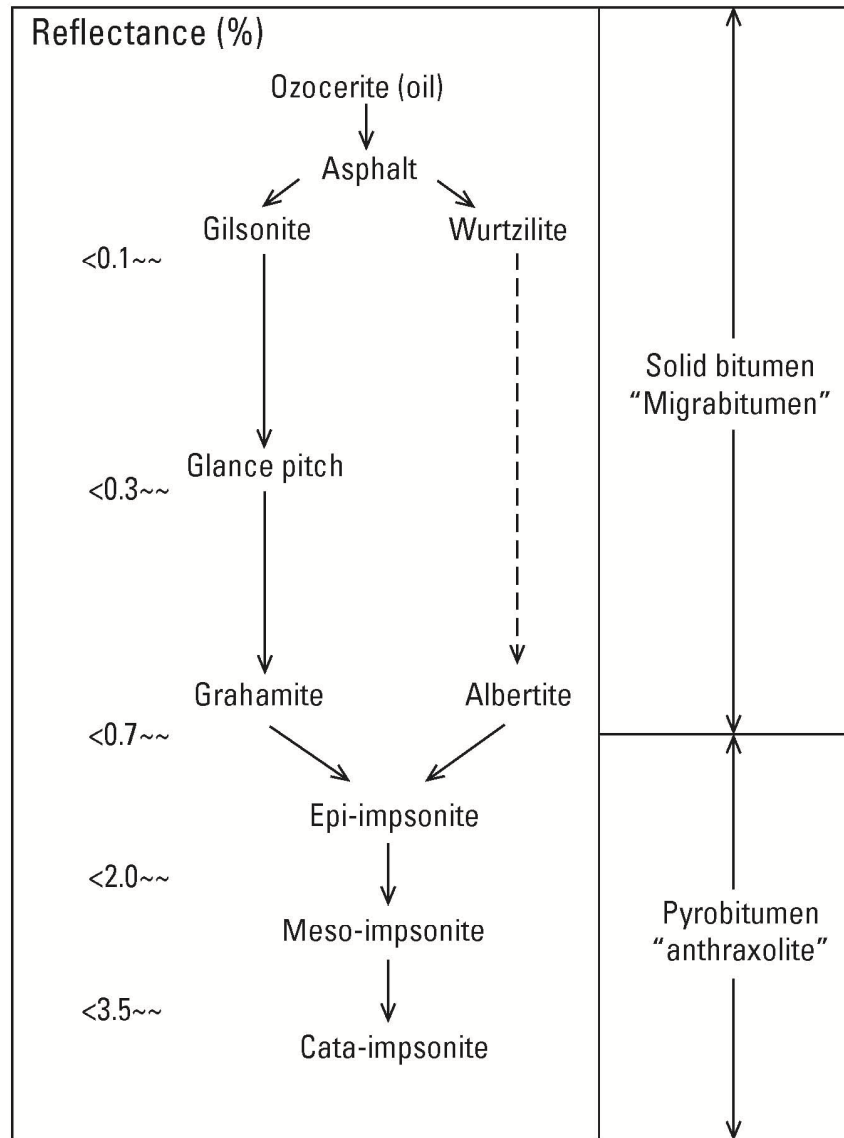


Figure 14

Figure 14. Geologic cross-section along transect D showing the distribution of measured Devonian shale  $R_0$  values and projected subsurface Devonian shale  $R_0$  and Pennsylvania coal  $R_{0(max)}$  isograds based on map view isograds from Repetski et al. (2008) and Ruppert et al. (2010), respectively. HGS, Humble Geochemical Services.



**Figure 15**

Figure 15. Classification of solid hydrocarbons. From Landis and Castaño (1995) and Jacob (1989).

## Gas Chromatographic Analysis of Bitumen Extracts

### Concept and Methodology

Oil and (or) gas in Devonian black shales of the Appalachian Basin mainly is generated from a mixture of bituminite and laminated alginite (amorphous organic matter; type II kerogen) having abundant high molecular weight *n*-alkanes. As Devonian black shale advances through the thermal maturation process the distribution of the *n*-alkane spectrum changes according to the level of thermal maturation. Thus, lower molecular weight *n*-alkanes (*n*-C<sub>12</sub> to *n*-C<sub>18</sub>) in the whole-oil GC spectrum increase in relative abundance at the expense of higher molecular weight *n*-alkanes (*n*-C<sub>19</sub> to *n*-C<sub>30+</sub>) because of thermal cracking processes associated with increasing thermal maturity. For example, in the Appalachian and Illinois basins, bitumens extracted from thermally immature Devonian shale show a broad GC spectrum with abundant high molecular weight *n*-alkanes, whereas bitumens extracted from thermally mature Devonian shale show a narrow GC spectrum with more moderate amounts of high molecular weight *n*-alkanes (Figure 16). Also, the relative abundance of high molecular weight *n*-alkanes in immature or low maturity samples produces a gently sloping spectrum with a broad secondary shoulder, whereas relative absence of high molecular weight *n*-alkanes in higher maturity samples produces a steeply sloping GC spectrum. Although the Illinois Basin example with a broad secondary shoulder for an immature sample is based on a GC from an oil sample, the same results are expected for a GC from a bitumen extract.

Three qualitatively derived types of GC spectra for bitumen extracts are described according to their level of thermal maturity. Level one, shown by a solid yellow circle on Figure 17, has a broad GC spectrum with one or more shoulders and characterizes an immature to marginally mature sample with respect to oil and (or) gas generation. Level two, indicated by a solid red circle, has a narrow GC spectrum and characterizes a mature sample (probably oil- and early-gas stage of maturation). Level three is indicated by a solid brown circle, has an unresolved “hump” of higher molecular weight components, and identifies a mature sample with respect to oil and (or) gas generation (probably gas- and latest-oil stage of maturation). GCs from 36 bitumen extract samples from 32 drill holes along transects A-D were classified according to their thermal maturity level and plotted on the cross-sections (Figures 18, 19, 20, and 21) and plan view map (Figure 22) according to the color codes shown on Figure 17. Several GCs cannot be evaluated because they show spurious high molecular weight *n*-alkane peaks that probably were introduced to the sample as a contaminant such as a drilling fluid additive.

Ground shale samples (~10 g, 60 mesh, 0.25 mm top size) were extracted at Weatherford Laboratories via reflux in Soxhlet with dichloromethane in the presence of activated Cu. Extraction continued overnight or until extracts ran clear. Extracts were filtered through Whatman No. 40 filters and solvent reduced through evaporation. Whole extracts were analyzed using an Agilent 6890N GC with injector held at 275°C. The GC was equipped with an Agilent DB-1 column (60 m, 0.25 mm i.d., 0.25 μm film thickness 100% dimethylpolysiloxane) using He as carrier gas. The column oven temperature program was 30°C (for 5 min), then increased by 3°C/min to 320°C (held for 20 min). Eluted components were identified by flame ionization detector held at 350°C.

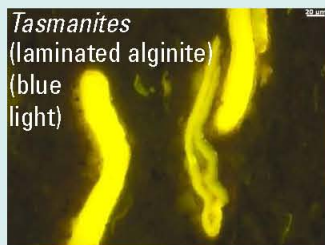
## Results

Estimated thermal maturity level along transects A-D based on GC character of extracted bitumens was plotted on the associated cross-sections and compared with the previously described Devonian shale  $R_o$  0.5 % and Pennsylvanian coal  $R_{o(max)}$  0.6 % isograds (Figures 18, 19, 20, and 21). Transect A clearly suggests that the boundary between immature Devonian shale samples (shown in yellow) and mature Devonian shale samples (shown in red) coincides with the Pennsylvanian coal  $R_{o(max)}$  0.6 % isograd and, therefore, is shifted about 100 mi westward of the onset of oil and (or) thermogenic gas generation originally defined by the shale  $R_o$  0.5 % isograd (Figure 18). In addition, transect A Lake Erie Shoreline shows that Devonian shale in drill hole  $A_{Lake}$  is immature and Devonian shale in drill hole  $A_{Ash}$  is very near the immature-mature boundary. In transect B, the boundary between immature Devonian shale and mature Devonian shale does not coincide exactly with the Pennsylvanian coal  $R_{o(max)}$  0.6 % isograd, but the match is reasonably close and is shifted about 15 mi westward of the onset of oil and (or) thermogenic gas generation originally defined by the shale  $R_o$  0.5 % isograd (Figure 19). Transect C shows the greatest disparity between immature-mature Devonian shale and the Pennsylvanian coal  $R_{o(max)}$  0.6 % isograd (Figure 20). Although the approximate limit of oil and (or) thermogenic gas generation (based on bitumen extract GCs) is shifted about 25 mi westward of the shale  $R_o$  0.5 % isograd, this boundary remains offset significantly (about 35 mi) from the Pennsylvanian coal  $R_{o(max)}$  0.6 % isograd. The Devonian shale  $R_o$  0.5 % and Pennsylvanian coal  $R_{o(max)}$  0.6 % isograds are closely matched on transect D (Figure 21); so there is no difficulty in selecting the western limit of oil and (or) thermogenic gas generation. However, Devonian shale  $R_o$  values associated with drill holes  $D_4$  and  $D_5$  are anomalously low for the corresponding Pennsylvanian coal  $R_{o(max)}$  isograds (Figure 14). This discrepancy is resolved with bitumen extract GCs which show Devonian shales in drill holes  $D_4$  and  $D_5$  to be mature with respect to oil and (or) thermogenic gas generation (Figure 21).

## Discussion

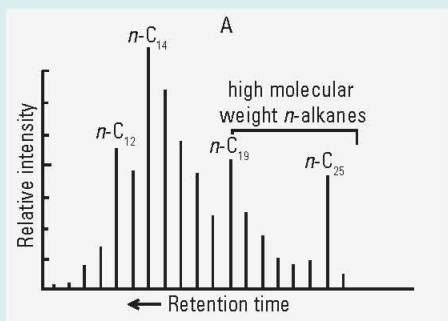
The distribution of thermal maturity levels along transects A-D and A Lake Erie Shoreline based on the spectral character of GCs of extracted bitumen is summarized in Figure 22. The key observation regarding the map patterns occurs along transect A where onset of oil and (or) thermogenic gas shown by the yellow-red boundary is shifted about 50 mi west of the Devonian shale  $R_o$  0.5 % isograd and is aligned with the Pennsylvanian coal  $R_{o(max)}$  0.6 % isograd. This shift implies that Devonian shale  $R_o$  values were underestimated in drill holes  $A_4$ - $A_6$  and that GC character of extracted bitumen provides a more accurate estimate of the boundary between thermally immature and mature Devonian shale. In contrast, transects B-D show no dramatic shifts of the immature-mature boundary (derived from GC spectral character of extracted bitumen) away from the Devonian shale  $R_o$  0.5 % isograd. Transect B shows little improvement in the definition of the immature-mature boundary because sample  $B_3$  is interpreted to be immature based on the GC character of extracted bitumen (Figure 19). Thus, the immature-mature boundary still is located approximately between drill holes  $B_3$  and  $B_4$  and misaligned with the Pennsylvanian coal  $R_{o(max)}$  0.6 % isograd. Although transect C shows a westward shift of the immature-mature boundary of about 30 mi from the location of the Devonian shale  $R_o$  0.5 % isograd, this shift still falls short of the Pennsylvanian coal  $R_{o(max)}$  0.6 % isograd by 50-60 mi. In transect D, analysis of GC spectra defines a immature-mature boundary consistent with the Devonian shale  $R_o$  0.5 % and Pennsylvanian coal  $R_{o(max)}$  0.6 % isograds, and suggests the Devonian shale is mature in drill holes  $D_4$  and  $D_5$  where  $R_o$  values indicate it is immature.

## Dominant organic matter in immature Devonian shale

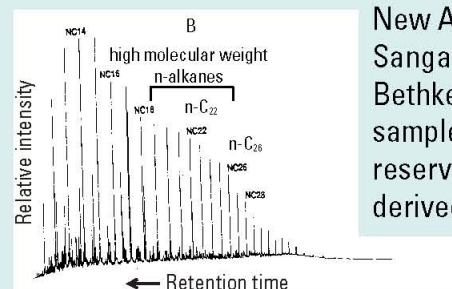


## GCs of extracted bitumen in immature Devonian shale

Higher molecular weight *n*-alkanes in the bitumen are present



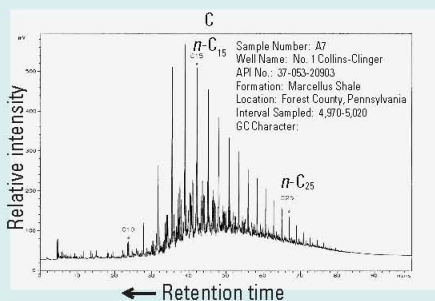
Lower Huron Shale  
Logan Co., Ohio  
McLaughlin et al. (1987), core sample



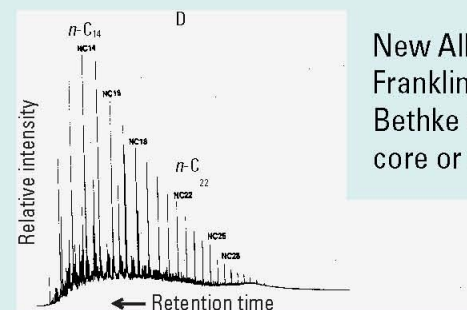
New Albany Shale  
Sangaman Co., Ill.  
Bethke et al. (1990), oil sample, (Silurian reservoirs, locally derived?)

## GCs of extracted bitumen in mature Devonian shale

Higher molecular weight *n*-alkanes in the bitumen are less abundant



Marcellus Shale  
Forest Co., Pa.  
drill hole A<sub>7</sub> of this report (see table 1), cuttings

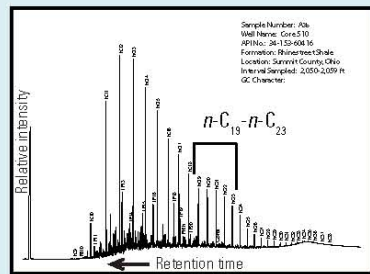
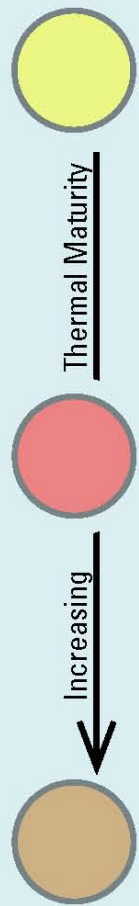


New Albany Shale  
Franklin Co., Ill.  
Bethke et al. (1990), core or cuttings

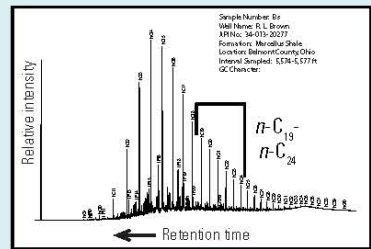
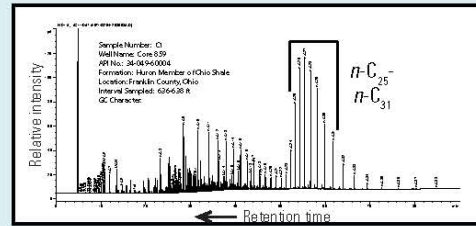
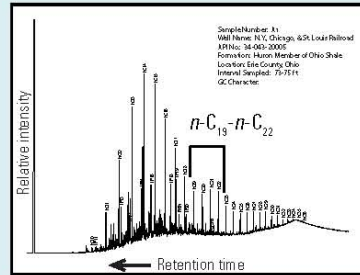
Increasing Thermal Maturity

**Figure 16**

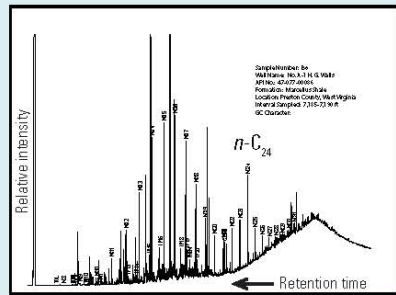
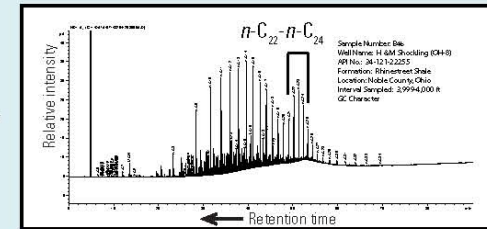
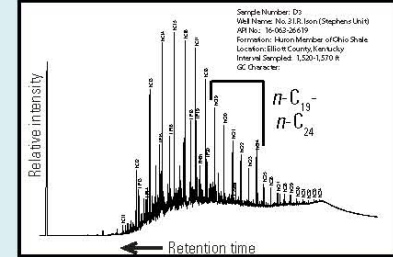
Figure 16. Contrasting changes in the spectral character of gas chromatograms of extracted bitumen between immature and thermally mature Devonian shales in the Appalachian and Illinois basins.



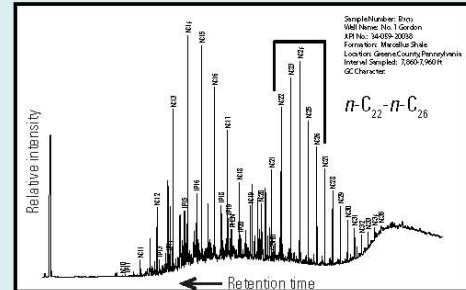
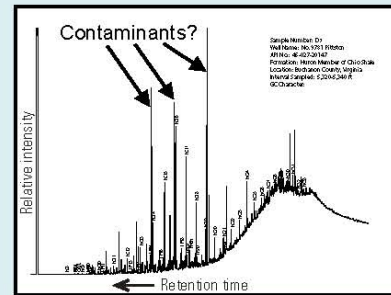
Broad spectrum with one or more shoulders of high molecular weight  $n$ -alkane peaks (several unexplained GCs with single  $n-C_{24}$  peak)



Bell-shaped spectrum with smooth slope of high molecular weight  $n$ -alkane peaks (several unexplained GCs with single  $n-C_{24}$  peak)



Partial spectrum with unresolved hump of high molecular weight  $n$ -alkane peaks (several unexplained GCs with single  $n-C_{24}$  peak)



Bimodal spectrum with high molecular weight  $n$ -alkane peaks (secondary peak may be caused by an additive to drilling fluid)

Figure 17

Figure 17. General changes in spectral character of Devonian shale bitumen extract GCs with increasing thermal maturity.

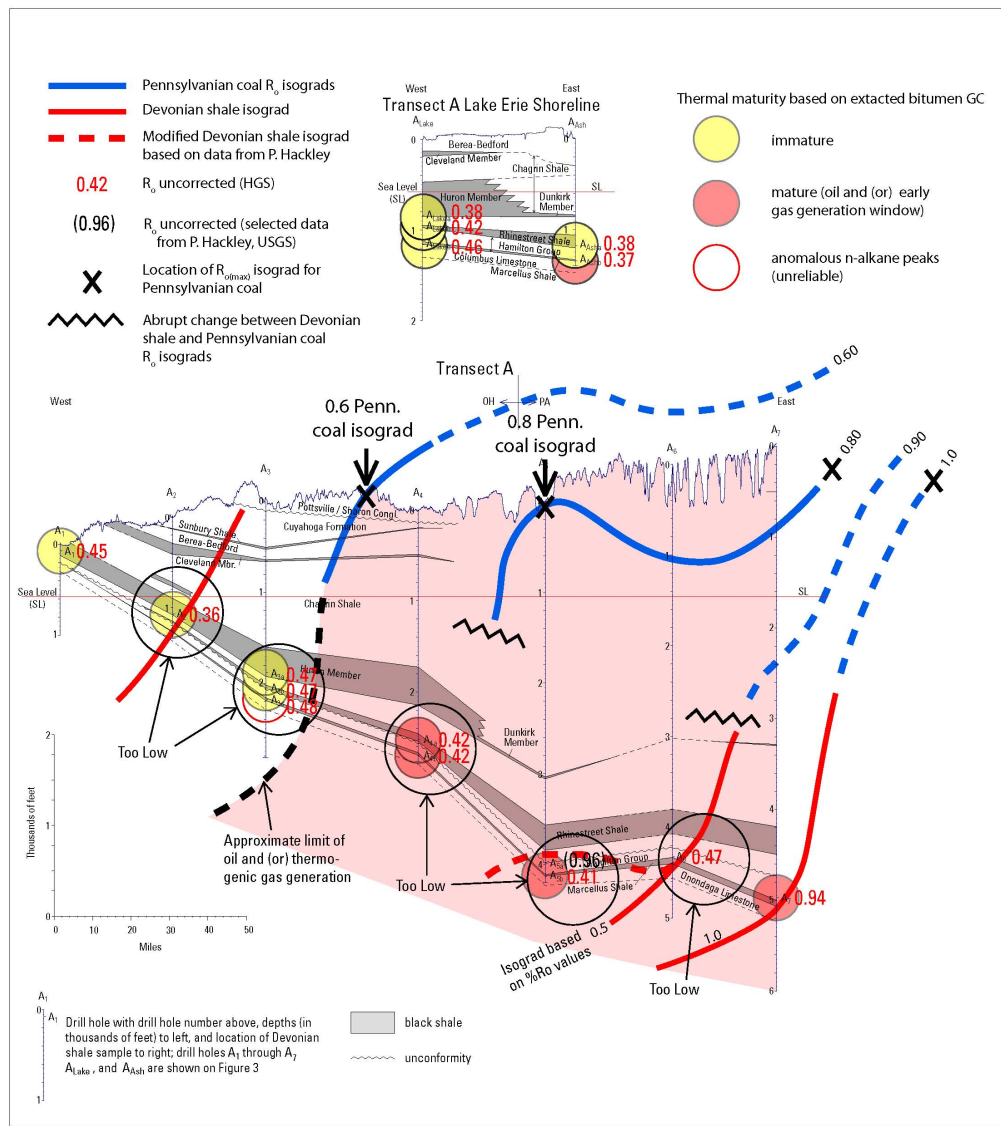


Figure 18

Figure 18. Geologic cross-sections along transects A and A Lake Erie Shoreline showing the stratigraphy and structure of Devonian black shales, subsurface distribution of shale  $R_o$  and Pennsylvanian coal  $R_{o(max)}$  isograds, and interpreted thermal maturity of shale based on spectral character of extracted bitumen.

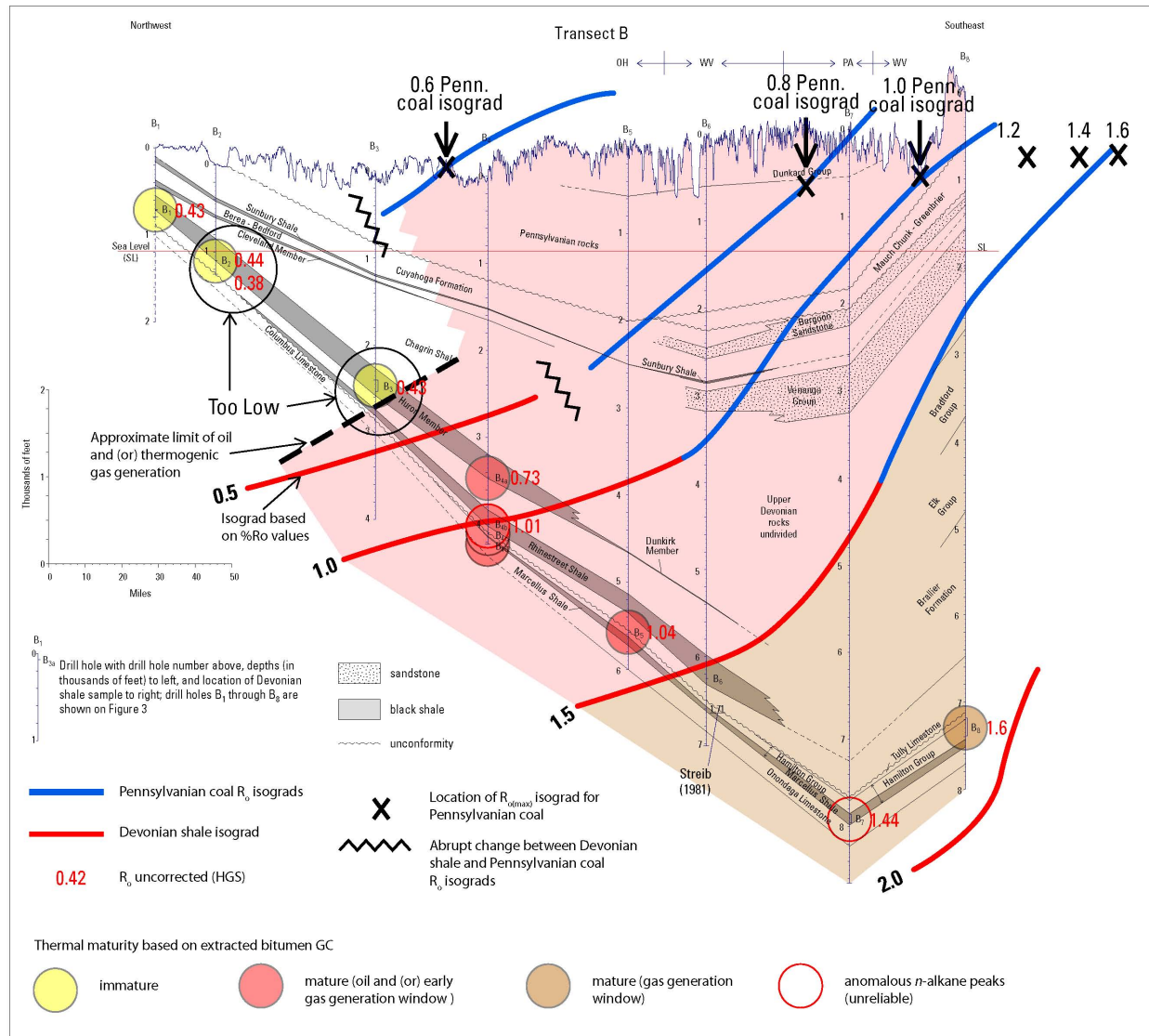
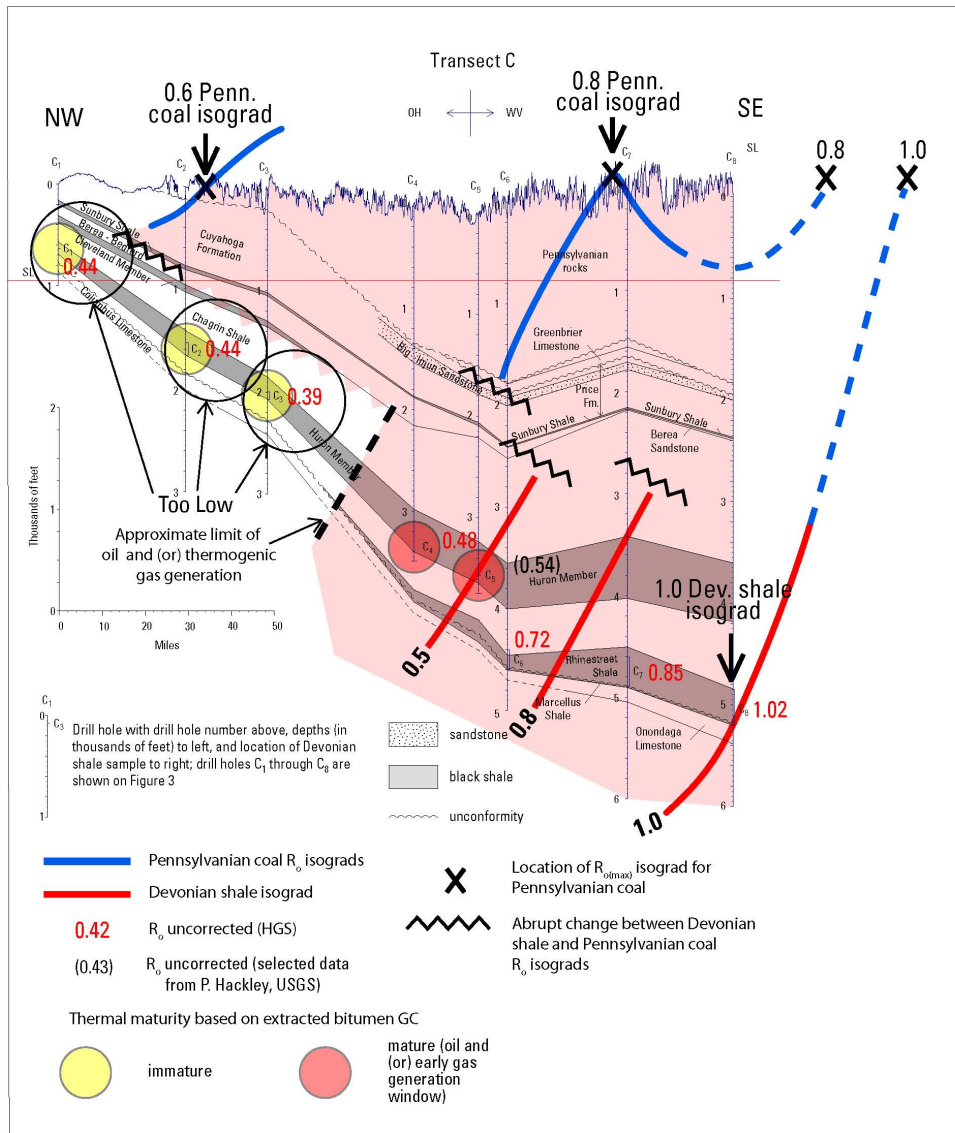


Figure 19

Figure 19. Geologic cross-section along transect B showing the stratigraphy and structure of Devonian black shales, subsurface distribution of shale  $R_0$  and Pennsylvanian coal  $R_{0(max)}$  isograds, and interpreted thermal maturity of shale based on spectral character of extracted bitumen.



**Figure 20**

Figure 20. Geologic cross-section along transect C showing the stratigraphy and structure of Devonian black shales, subsurface distribution of shale  $R_0$  and Pennsylvania coal  $R_{0(max)}$  isograds, and interpreted thermal maturity of shale based on spectral character of extracted bitumen.

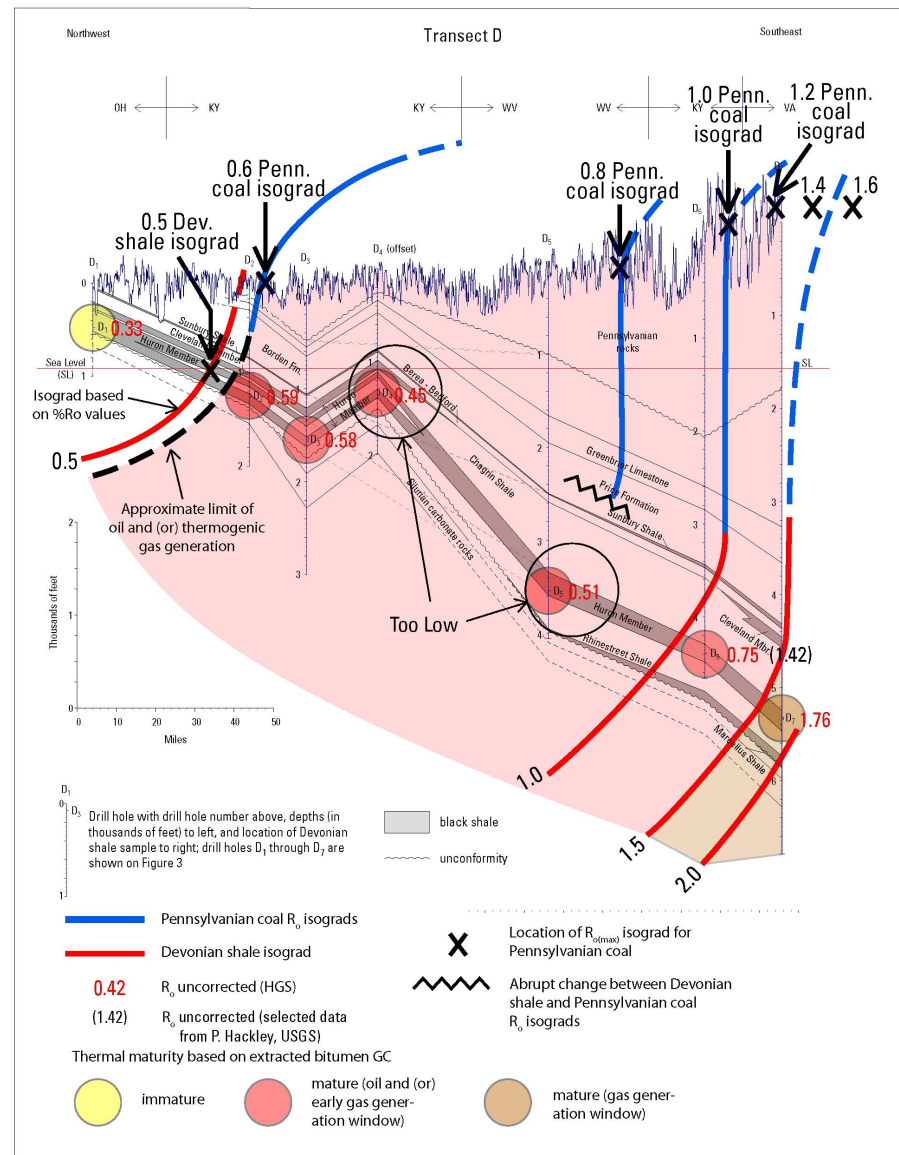


Figure 21

Figure 21. Geologic cross-section along transect D showing the stratigraphy and structure of Devonian black shales, subsurface distribution of shale  $R_0$  and Pennsylvanian coal  $R_{0(max)}$  isograds, and interpreted thermal maturity of shale based on spectral character of extracted bitumen.

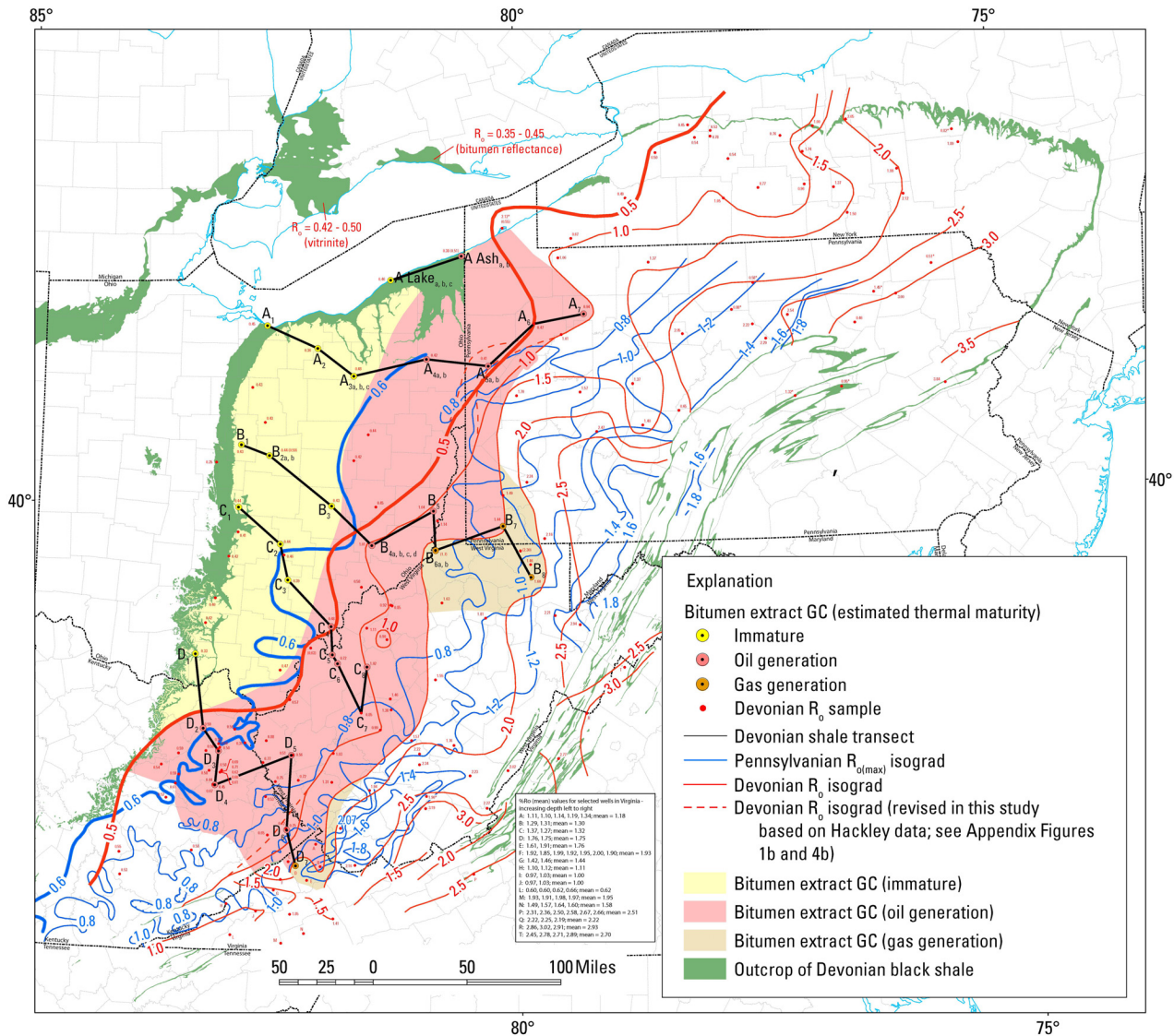


Figure 22

Figure 22. Index map showing the distribution of thermal maturity levels on transects A-D and A Lake Erie Shoreline based on the spectral character of GCs of bitumen extracts from Devonian shales.

## Dispersed Maceral Types and Spectral Fluorescence of *Tasmanites*

### Concept and Methodology

Dispersed macerals in Devonian shales gradually are converted from original bituminite and alginite source material (Type II kerogen) to petroleum and refractory residues with increasingly higher levels of thermal maturity. For example, samples containing abundant bituminite and alginite are considered to be thermally immature, whereas samples containing abundant solid bitumen (e.g., asphalt) are considered to represent a higher level of thermal maturity, probably within the stage of oil generation ([Figure 23](#)). Samples containing pyrobitumen are considered to have achieved an even higher level of thermal maturity that probably represents the stage of wet- and (or) dry-gas generation. Barrows and Cluff (1984) successfully used this approach to determine the onset of the oil window in the Devonian New Albany Shale in the Illinois Basin.

Spectral fluorescence characteristics of Devonian black shale rely on measurements of telalginite macerals (mainly derived from the alga *Tasmanites*). Samples having spectral fluorescence measurements with a mean  $\lambda_{\max}$ =575-600 nm are considered to be thermally mature (Teichmüller and Ottenjann, 1977; Robert, 1988). An example from drill hole C<sub>5</sub> in Jackson County, West Virginia ([Table 3](#)), with *Tasmanites*  $\lambda_{\max}$ =612 nm suggests that the sample is mature with respect to oil and (or) early thermogenic gas generation ( $R_o$ ~1.0 % according to Robert, 1988).

Spectral epi-fluorescence measurements were conducted at USGS with a Zeiss AxioImager microscope with a metal halide illuminator according to the calibration and methods described in Baranger et al. (1991). For each sample, ten measurements of the fluorescence spectrum of *Tasmanites* were collected using ultraviolet (356 nm) excitation. Spectral fluorescence data were determined to be accurate and reproducible through interlaboratory exercises in 2008-2010 on blind samples (Mendonça Filho et al., 2010).

### Results

The result of maceral type determinations and spectral fluorescence measurements along transects A-D and A Lake Erie Shoreline are reported in [Tables 1, 2, 3, and 4](#) and plotted on [Figure 24](#). Transect A shows that the  $\lambda_{\max}$ =600 nm contour coincides with the Pennsylvanian coal  $R_{o(\max)}$  0.6 % isograd, and, therefore, the onset of oil and (or) thermogenic gas generation is shifted about 50-60 mi westward of the onset of generation defined by the shale  $R_o$  0.5 % isograd. In addition, transect A Lake Erie Shoreline shows that Devonian shale in drill hole A<sub>Lake</sub> is largely immature ( $\lambda_{\max}$ =535 to 581 nm) and that shale in drill hole A<sub>Ash</sub> is very near the immature-mature boundary ( $\lambda_{\max}$ =567 to 592 nm). In transect B, the  $\lambda_{\max}$ =600 nm contour coincides approximately with the Pennsylvanian coal  $R_{o(\max)}$  0.6 % and Devonian shale  $R_o$  0.5 % isograds. Transect C shows the greatest disparity between the  $\lambda_{\max}$ =600 nm contour and the Pennsylvanian coal  $R_{o(\max)}$  0.6 % isograd. Although the approximate onset of oil and (or) thermogenic gas generation (based on the  $\lambda_{\max}$ =600 nm contour) is shifted about 10 mi westward of the shale  $R_o$  0.5 % isograd, this boundary remains offset significantly eastward (about 40 mi) of the Pennsylvanian coal  $R_{o(\max)}$  0.6 % isograd. In contrast to the other transects, transect D shows the onset of oil and (or) thermogenic gas generation (based on the  $\lambda_{\max}$ =600 nm contour) shifted eastward

about 40-50 mi of the shale  $R_o$  0.5 % and Pennsylvanian coal  $R_{o(max)}$  0.6 % isograds. Thus, maceral type determinations and spectral fluorescence measurements may underestimate the western limit of oil and (or) thermogenic gas generation on this transect.

## Discussion

Estimated thermal maturity level for each sample on transects A-D and A Lake Erie Shoreline based on maceral types and spectral fluorescence measurements was plotted on [Figure 24](#) and compared with the Devonian shale  $R_o$  0.5 % and Pennsylvanian coal  $R_{o(max)}$  0.6 % isograds. Although the distribution of identified maceral types and the  $\lambda_{max}=600$  nm isoline seem to be in general agreement, the  $\lambda_{max}=600$  nm contour provides a more consistent indicator of thermal maturity of Devonian shale. The best thermal maturity indicators of the macerals are amorphous kerogen (bituminite and alginite) and pyrobitumen where they appear, on the immature and mature sides of the  $\lambda_{max}=600$  nm contour, respectively. By comparison, bitumen is present in both the immature and mature sectors as suggested by the  $\lambda_{max}=600$  nm isograd. The key observation regarding spectral fluorescence measurements involves transect A where the onset of oil and (or) thermogenic gas (based on the  $\lambda_{max}=600$  nm contour) is shifted about 50 mi west of the Devonian shale  $R_o$  0.5 % isograd and is aligned with the Pennsylvanian coal  $R_{o(max)}$  0.6 % isograd. This shift may imply that Devonian shale  $R_o$  values may underestimate thermal maturity in drill holes A<sub>4</sub>-A<sub>6</sub>. Transect B shows no real change in the location of the onset of oil and (or) thermogenic gas because the  $\lambda_{max}=600$  nm contour coincides with the Devonian shale  $R_o$  0.5 % and Pennsylvanian coal  $R_{o(max)}$  0.6 % isograds. Although transect C shows a westward shift of about 10 mi for the onset of oil and (or) thermogenic gas generation (based on the  $\lambda_{max}=600$  nm contour) from the location of the Devonian shale  $R_o$  0.5 % isograd, this shift still falls well short of the Pennsylvanian coal  $R_{o(max)}$  0.6 % isograd. In transect D, distribution of maceral types and the  $\lambda_{max}=600$  nm contour define a thermal immature-mature boundary that is shifted 40 to 50 mi southeast of the shale  $R_o$  0.5 % and Pennsylvanian coal  $R_{o(max)}$  0.6 % isograds. This significant southeastward shift is inconsistent with the other transects and remains unexplained.

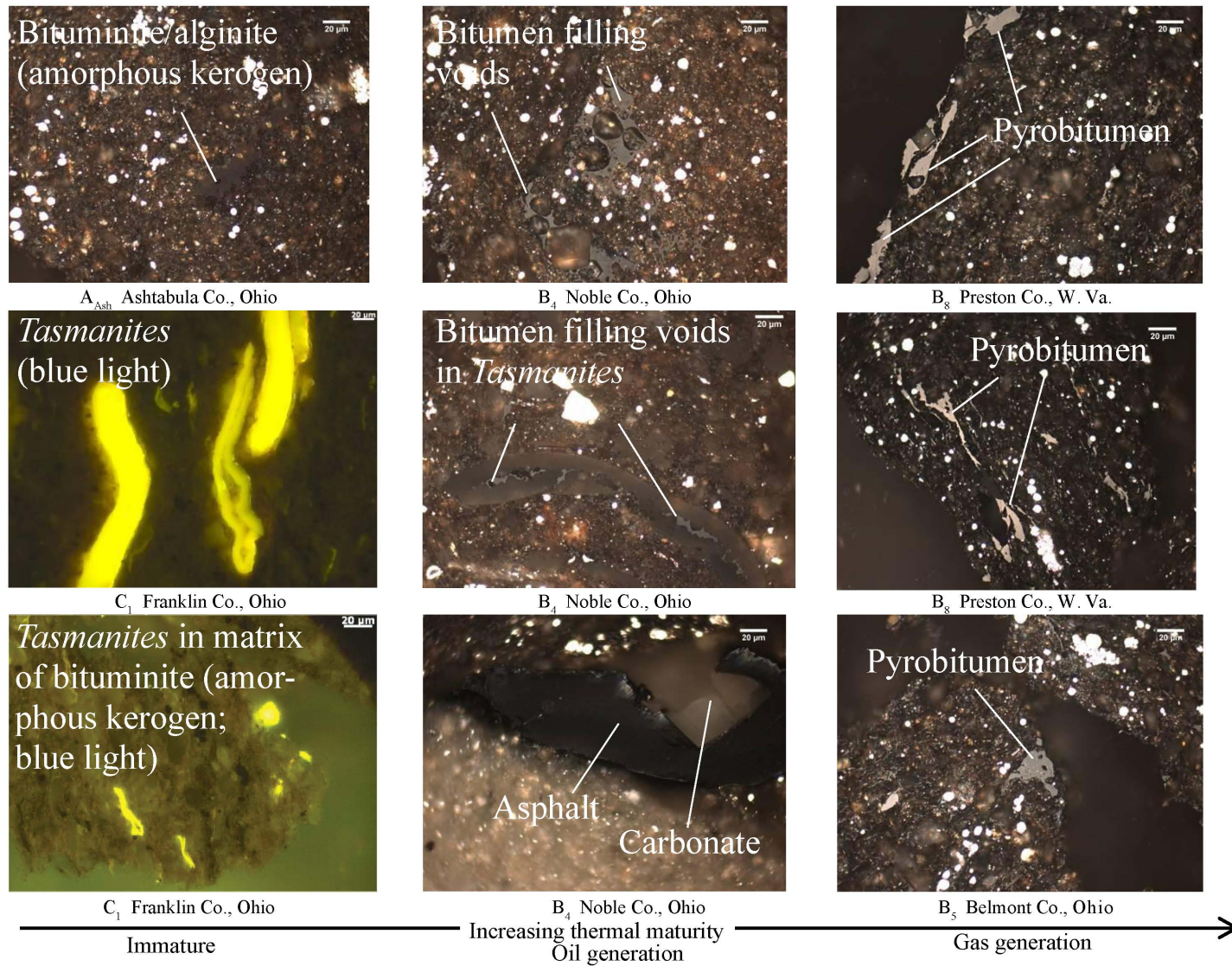


**Figure 23**

Figure 23. General changes in the character of dispersed macerals in Appalachian Basin Devonian shale with increasing thermal maturity.

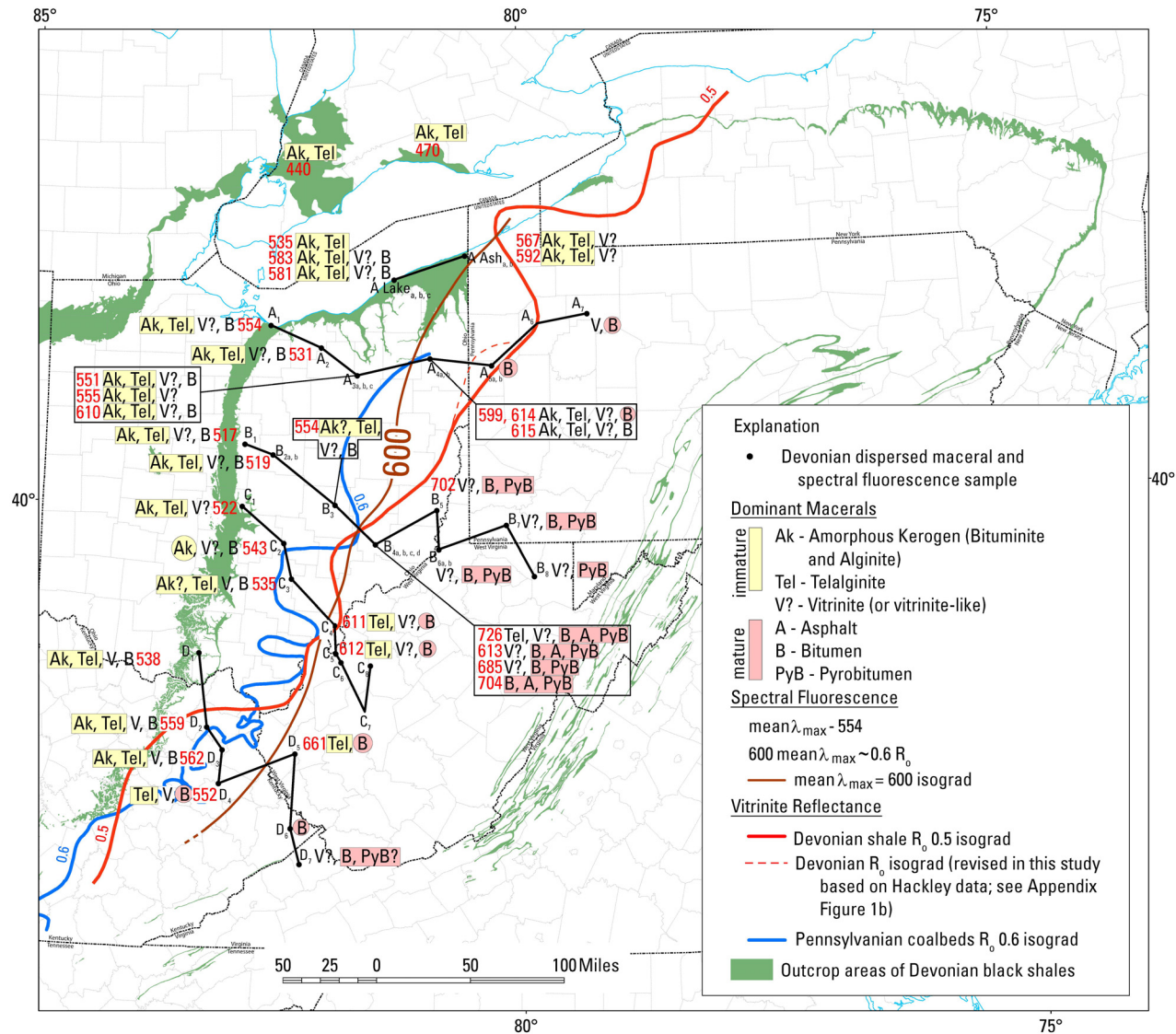


Figure 24

Figure 24. Index map showing the distribution of thermal maturity levels on transects A-D and A Lake Erie Shoreline based on dispersed maceral types and spectral fluorescence measurements.

## Hydrogen Index (HI) Contours

### Concept and Methodology

The Hydrogen Index (HI) (mg HC/g TOC) component of the Rock-Eval II analysis and the related atomic H/C ratio gradually decrease with thermal maturity and organic matter conversion to petroleum. Lewan et al. (2002) successfully used HI contouring to determine the onset of the oil window in the Devonian New Albany Shale in the Illinois Basin. Based on a calibration curve for the New Albany shale in the Illinois Basin where HI was plotted against atomic H/C ratio and mole fraction ( $H/[C+H]$ ), Lewan et al. (2002) interpreted the onset of petroleum generation to occur at HI = 400 mg HC/g TOC (Figure 25). The calibration curve of Lewan et al. (2002) that determined the 400 HI contour limit for the pod of active source rocks used samples having 2.5 wt.% or greater TOC to insure a continuous bitumen network. In the absence of a calibration curve for the Devonian shale of the Appalachian Basin, the New Albany Shale curve derived by Lewan et al. (2002) was applied in this investigation and the 400 HI contour was used to establish the onset of petroleum generation. Because the 2.5 wt.% or greater TOC requirement for the Appalachian Basin samples could not provide an adequate dataset, the requirement was decreased to 1.5 wt.% or greater TOC.

### Results

The HI data points (with 1.5 wt.% or greater TOC) used in this study were derived from the Repetski et al. (2008) database. The contoured hydrogen index (HI) values are plotted on Figure 26, and the HI values on transects A-D and Lake Erie Shoreline are compiled in Tables 1, 2, 3, and 4. Transect A shows that the HI=400 contour is closely aligned with the coal  $R_{o(max)}$  0.6 % isograd and, therefore, the onset of oil and (or) thermogenic gas generation is shifted about 35-40 mi westward from the shale  $R_o$  0.5 % isograd. In addition, transect A Lake Erie Shoreline shows that Devonian shale in drill hole  $A_{Lake}$  is immature (HI=227 (anomalous), 439, 475) and that shale in drill hole  $A_{Ash}$  is near the immature-mature boundary (HI=358, 434). In transect B, the HI=400 contour is shifted approximately 15 mi west of the coal  $R_{o(max)}$  0.6 % and shale  $R_o$  0.5 % isograds. Transects C and D show the greatest disparity between the HI=400 contour and the shale  $R_o$  0.5 % and coal  $R_{o(max)}$  0.6 % isograds. Although the approximate onset of oil and (or) thermogenic gas generation on transect C (based on the HI=400 contour) is shifted about 10 mi westward of the shale  $R_o$  0.5 % isograd, this is significantly offset (about 40 mi) from the coal  $R_{o(max)}$  0.6 % isograd. The onset of oil and (or) thermogenic gas generation (based on the HI=400 contour) on transect D is shifted eastward about 40 mi from the shale  $R_o$  0.5 % isograd and about 30 mi from the coal  $R_{o(max)}$  0.6 % isograd. Thus, the HI=400 contour in this transect may not adequately estimate the western limit of oil and (or) thermogenic gas generation.

### Discussion

A key observation regarding Figure 26 involves transect A where the onset of oil and (or) thermogenic gas (based on the HI=400 contour) is shifted about 50 mi west of the shale  $R_o$  0.5 % isograd and is nearly aligned with the coal  $R_{o(max)}$  0.6 % isograd. This shift implies that the shale  $R_o$  % values may underestimate thermal maturity in drill holes  $A_4$ - $A_6$  and that the HI=400 contour may provide a more accurate estimate of the boundary between thermally immature and mature Devonian shale. Transect B shows a similar westward shift of the onset of oil and (or)

thermogenic gas (based on the HI=400 contour) in comparison to the shale  $R_o$  0.5 % isograd. However, the westward shift is less dramatic (about 15 mi). This westward shift of the onset of oil and (or) thermogenic gas (based on the HI=400 contour) on transect B suggests that the shale  $R_o$  values may underestimate thermal maturity in drill hole B<sub>3</sub> and that the HI=400 contour may provide a more accurate estimate of the boundary between thermally immature and mature shale. Transect C also shows a westward shift of the onset of oil and (or) thermogenic gas (based on the HI=400 contour), but the shift is only about 10 mi from the shale  $R_o$  0.5 % isograd and falls well short of the coal  $R_{o(max)}$  0.6 % isograd. In transect D, the location of the HI=400 contour defines a thermal immature-mature boundary that is shifted 40 to 50 mi southeast of the shale  $R_o$  0.5 % and coal  $R_{o(max)}$  0.6 % isograds. This significant southeastward shift is unexplained.

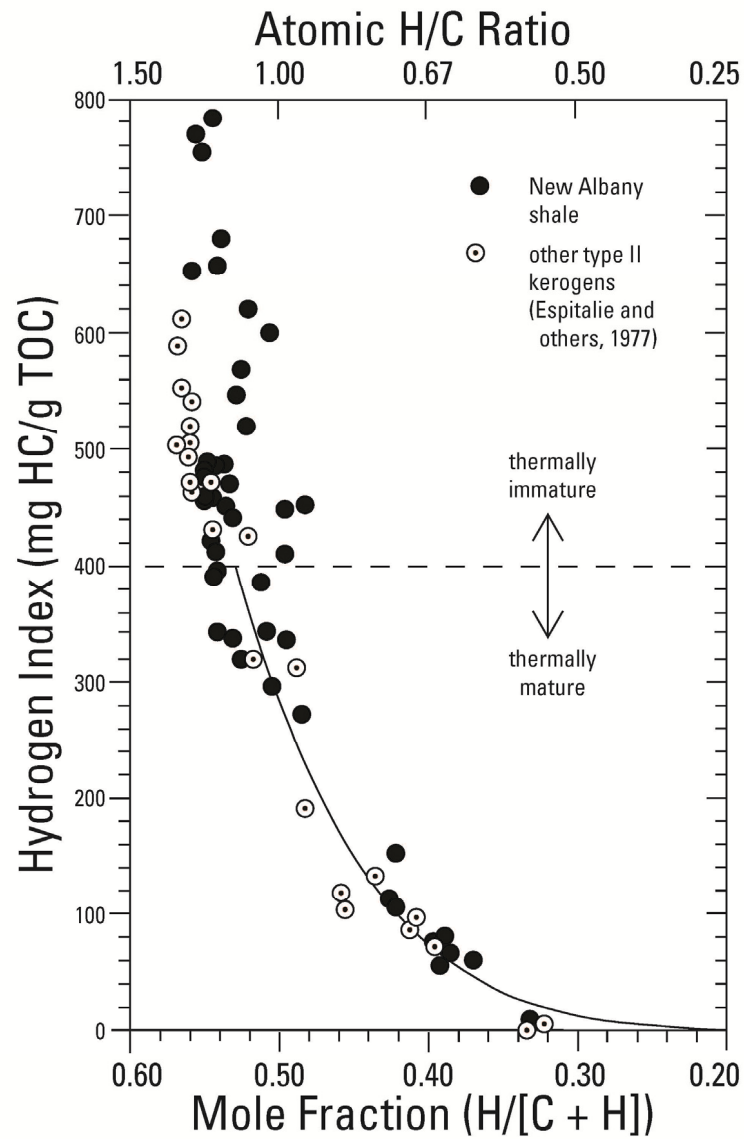


**Figure 25**

Figure 25. Hydrogen Index (HI; mg HC/g TOC) from Rock-Eval pyrolysis plotted against atomic H/C ratio and mole fraction (H/[C+H]) for samples of the New Albany Shale in the Illinois Basin (Lewan et al., 2002).

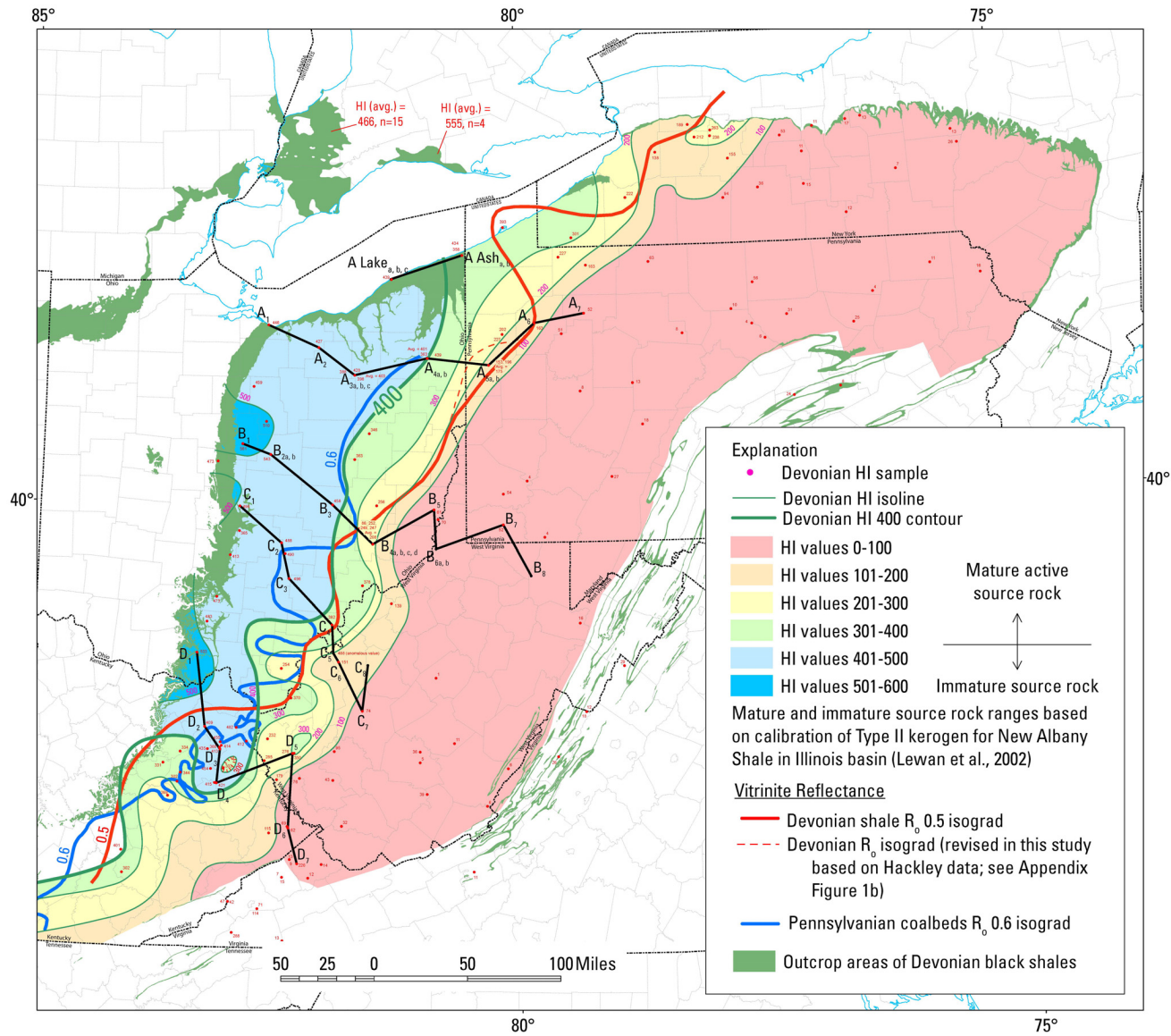


Figure 26

Figure 26. Index map showing the distribution of HI contours along transects A-D and A Lake Erie Shoreline.

## Summary, Conclusions, and Follow-up Studies

The three key boundaries or contour lines used herein to discriminate between immature versus mature regions of Devonian shale are summarized on [Figure 27](#) and include, as discussed: 1) differences in the GC spectral distributions of extracted bitumen (marked GC Immature-Mature), 2) the  $\lambda_{\max}=600$  nm contour line derived from spectral fluorescence measurements of *Tasmanites*, and 3) the HI=400 contour line derived from Rock-Eval data. All three boundaries are considered to demonstrate where the onset of oil and (or) thermogenic gas occurs. In eastern Ohio, western Pennsylvania, and northern West Virginia the three boundary lines are reasonably close together and coincide approximately with the Pennsylvanian coal  $R_{o(\max)}$  0.6 % isograd. The width of the zone that encompasses the three boundary and contour lines (shown by the shaded yellow band) is relatively narrow and ranges from 10 to 25 mi wide. In eastern Kentucky, southern Ohio, and southern West Virginia the three boundaries are less well constrained to a common zone and range from 30-50 mi apart. Although the zone that is common to the three key boundaries is relatively wide in the south, it does confine most of the coal  $R_{o(\max)}$  0.6 % isograd.

The analysis presented herein suggests that the three Devonian black shale parameters (GC character,  $\lambda_{\max}=600$  nm, HI=400 mg HC/g TOC) are plausible indicators of the onset of oil and (or) thermogenic gas generation and that they may be more reliable than the Devonian shale  $R_o$  0.5 % isograd shown by Repetski et al. (2008), particularly in the northern part of our study area. In the southern part of the study area the three parameters are plausible thermal-maturity indicators, but the results are less convincing. The inability of these three parameters to mimic the thermal maturity level commensurate with the coal  $R_{o(\max)}$  isograd along transects C and D is inexplicable and may be related to kerogen type, data gaps, or problems with data quality in certain areas. One dilemma these new data present is how to decide which parameter presents the best independent measure of the onset of oil and (or) thermogenic gas generation in low thermal maturity shale. One solution is to map the updip and downdip boundaries of the area that confines the three isolines and report that initial hydrocarbon generation falls somewhere in between.

A comparison of the boundary of immature-mature Devonian shale using the three parameters evaluated in this report with the Devonian shale  $R_o$  (corrected) boundary used by Milici et al. (2011) suggests that the  $R_o$  (corrected) boundary in Ohio is located 60-70 mi farther westward than the maturity limits defined herein ([Figure 27](#)). Also, modeling studies by Rowan (2006) in northern Ohio showed that the immature-mature Devonian shale boundary is located 10-40 mi farther westward than the maturity limits defined herein. The western limits of Devonian shale petroleum generation as determined by Milici et al. (2011) and Rowan (2006) are considered unrealistic for Ohio because of their large variance with the maturity limits rigorously defined in this report. However, in eastern Kentucky, the Devonian shale  $R_o$  (corrected) boundary used by Milici et al. (2011) falls within the zone of petroleum generation as defined in this report and, thus, is considered to be more realistic than the  $R_o$  (corrected) boundary in Ohio.

One conclusion of this work is that the  $R_o=0.5$  % isograd of Repetski et al. (2008) is too conservative because it is based largely on measurement of the reflectance of solid bitumen. Moreover, the term “vitrinite suppression” may not be applicable because the predominant maceral is solid bitumen, and, therefore, samples corrected for vitrinite suppression may produce inconsistent and “artificial”  $R_o$  values. Hackley et al. (in press) used biomarker ratios to demonstrate that  $R_o$  underestimates thermal maturity in the low maturity areas on the same transects of the current study area and also concluded that this was because of the misidentification of solid bitumen as vitrinite.

Another conclusion is that GC analysis of extracted bitumen, identification of dispersed maceral types and the spectral fluorescence of *Tasmanites*, and Hydrogen Index (HI) contours all appear to be better predictors than  $R_o$  for the updip limit of mature Devonian shale source rocks. Probably, the HI contour method may be the easiest test to perform because it is the least labor intensive and least expensive. However, a dataset of Appalachian black shale samples must be collected and analyzed to calibrate the Rock-Eval derived HI vs. atomic H/C ratios as was done in the Illinois Basin by Lewan et al. (2002).

Several follow-up studies may improve the reliability of the geochemical- and maceral-based tests evaluated here. Anomalous peaks (probably contaminants) noted in the whole extract GCs should be identified to better understand the GC spectra in the context of their thermal maturity setting. Isotope geochemistry of gases in Devonian shale reservoirs along transects A-D and A Lake Erie Shoreline might corroborate the thermal maturity boundaries and contour lines defined in this study. Finally, there is one general question applicable to the Devonian shales of this study and to black shale intervals in other basins: why have type II kerogen-bearing, oil-prone source rocks generated natural gas rather than oil in low maturity parts of the basin? In other words, the hydrocarbon phase that is accumulated spatially near to the onset of petroleum generation at thermal maturity levels of  $R_o=0.5$  to  $0.6$  % is most commonly gas, not oil, based on visual evaluation of Devonian-reservoired hydrocarbons shown on the oil and gas fields of Ohio map (Baranoski, 1996). Some liquids may accompany the gases generated at these low maturity levels, but commonly the gas is dry and thermogenic in origin according to isotopic data (e.g., Osborn and McIntosh, 2010). Perhaps early expelled mobile oil has migrated out of the source rock, leaving abundant mobile gas tightly held within the shale matrix with residual oil. Another factor could be that the thermogenic dry gas has migrated into shale reservoirs from deeper in the basin, although Ryder (2008) considered this scenario unlikely because of thick, widespread impervious Silurian evaporites.

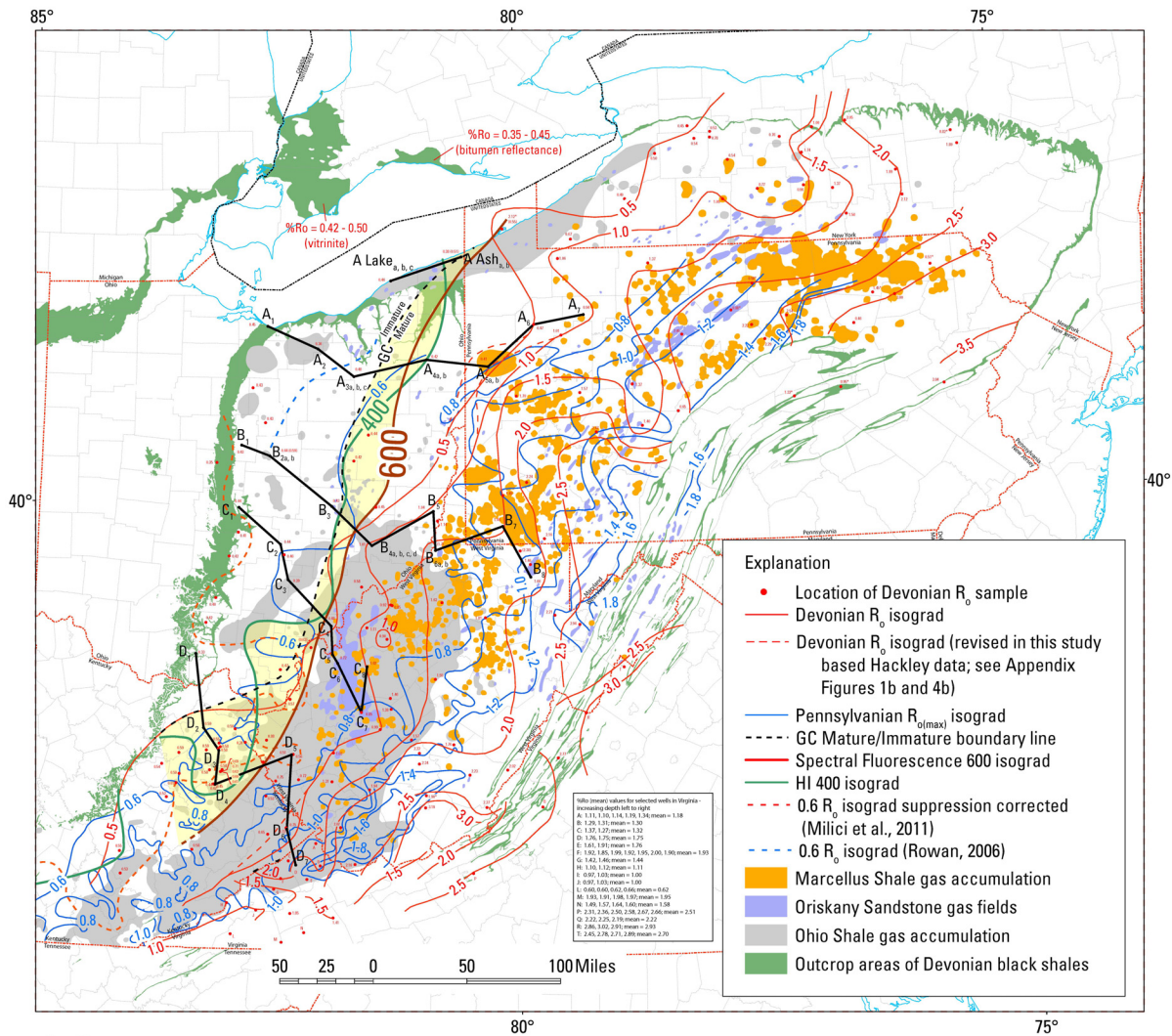


Figure 27

Figure 27. Summary map of the study area showing the distribution of the immature-mature boundary of Devonian shales along transects A-D and A Lake Erie Shoreline based on analysis of GC spectral character, spectral fluorescence of *Tasmanites* algae, and HI. Also shown are immature-mature boundaries of Devonian shale based on burial history modeling studies by Rowan (2006), and suppression-corrected  $R_0$  data from Milici et al. (2011).

## Acknowledgements

Reviews by Catherine B. Enomoto and Robert C. Milici of USGS improved the manuscript. Any use of trade, product, or firm names herein is for descriptive purposes only and does not imply endorsement by the U.S. Government.

## References Cited

ASTM, 2011a, D2797/D2797M-11a Standard practice for preparing coal samples for microscopical analysis by reflected light: Annual Book of ASTM Standards: Petroleum Products, Lubricants, and Fossil Fuels; Gaseous Fuels; Coal and Coke, sec. 5, v. 5.06: ASTM International, West Conshohocken, PA, p. 454-458.

ASTM, 2011b, D7708-11 Standard test method for microscopical determination of the reflectance of vitrinite dispersed in sedimentary rocks: Annual book of ASTM standards: Petroleum products, lubricants, and fossil fuels; Gaseous fuels; coal and coke, sec. 5, v. 5.06: ASTM International, West Conshohocken, PA, p. 823-830.

Baranger, R., L. Martinez, J.-L. Pittion, and J. Pouleau, 1991, A new calibration procedure for fluorescence measurements of sedimentary organic matter: *Organic Geochemistry*, v. 17, p. 467-475.

Baranoski, M.T., 1996, Oil and gas fields of Ohio, 1996: Ohio Division of Geological Survey, Digital Chart and Map Series DCMS-21, scale 1:1,000,000.

Barker, C.E., M.D. Lewan, and M.J. Pawlewicz, 2007, The influence of extractable organic matter on vitrinite reflectance suppression: a survey of kerogen and coal types: *International Journal of Coal Geology*, v. 70, p. 67-78.

Barrows, M.H., and R.M. Cluff, 1984, New Albany Shale Group (Devonian-Mississippian) source rocks and hydrocarbon generation in the Illinois Basin, *in* G. Demaison, and R.J. Murvis, eds., *Petroleum geochemistry and basin evolution*: Tulsa, Oklahoma, AAPG Memoir 36, p. 111-138.

Bethke, C.M., J.D. Reed, and D.F. Oltz, 1990, Long-range petroleum migration in the Illinois Basin, *in* M. W. Leighton, D. R. Kolata, D. F. Oltz, and J. J. Eidel, eds., *AAPG Memoir 51*, p. 455-472.

Carr, A. D., 2000, Suppression and retardation of vitrinite reflectance, part 1: Formation and significance for hydrocarbon generation: *Journal of Petroleum Geology*, v. 23, p. 313-343.

Cliffs Minerals, Inc., 1979a, Eastern Gas Shales Project, Ohio well #4: Cliffs Minerals, Inc., Phase I Report, Field Operations [August 1979], unpaginated.

- Cliffs Minerals, Inc., 1979b, Eastern Gas Shales Project, Ohio well #5: Cliffs Minerals, Inc., Phase I Report, Field Operations [September 1979], unpaginated.
- Curiale, J.A., 1986, Origin of solid bitumens, with emphasis on biological marker results: *Organic Geochemistry*, v. 10, p. 559-580.
- Espitalié, J.M., J.L. Laporte, M. Madec, F. Marquis, P. Leplat, J. Paulet, and A. Boutefeu, 1977, Methode rapide de caracterisation des roches meres de leur potential petrolier et de leur degre d' evolution: *Revue de l'Institute Français du Pétrole*, v. 32, p. 23-42.
- ExLog Brown and Ruth Laboratories, Inc., 1988, Geochemical Data—Ohio: GRI Contract 5085-213-1181, unpaginated.
- Hackley, P.C., R.T. Ryder, M.H. Trippi, and H. Alimi, 2013, Thermal maturity of northern Appalachian Basin Devonian shales: insights from sterane and terpane biomarkers: *Fuel*, v. 106, p. 445-462,
- Hutton, A.C., and A.C. Cook, 1980, Influence of alginite on the reflectance of vitrinite: *Fuel*, v. 59, p. 711-716.
- Jacob, H., 1989, Classification, structure, genesis and practical importance of natural solid oil bitumen (—migrabiten"): *International Journal of Coal Geology*, v. 11, p. 65-79.
- Koppe, E.F., 1959, Grahamite dikes in the Pittsburgh coal, Washington County, Pennsylvania [abs]: *Geological Society of America Bulletin*, v. 70/12, pt. 2, p. 1632.
- Landis, C.R., and J.R. Castaño, 1995, Maturation and bulk chemical properties of a suite of solid hydrocarbons: *Organic Geochemistry*, v. 22/1, p. 137-149.
- Lewan, M.D., M.E. Henry, D.H. Higley, and J.K. Pitman, 2002, Material-balance assessment of the New Albany-Chesterian petroleum system of the Illinois Basin: *AAPG Bulletin*, v. 86/5, p. 745-778.
- Lo, H.B., 1993, Correction criteria for the suppression of vitrinite reflectance in hydrogen-rich kerogens: preliminary guidelines: *Organic Geochemistry*, v. 20/6, p. 653-657.
- Majchszak, F.L., 1980, Borehole geophysical-log correlation network for Devonian shales in eastern Ohio: stratigraphic cross-section D-D': Ohio Division of Geological Survey map, Morgantown Energy Technology Center (METC)/Eastern Gas Shales Project (EGSP) Series 307, 2 sheets.
- McLaughlin, J.D., R.L. McLaughlin, and W.A. Kneller, 1987, Organic geochemistry of the kerogen and bitumen from the Ohio Shale by pyrolysis-gas chromatography: *International Journal of Coal Geology*, v. 7, p. 21-51.

McTavish, R.A., 1998, The role of overpressure in the retardation of organic matter maturation: *Journal of Petroleum Geology*, v. 21, p. 153-186.

Mendonça Filho, J.G., C.V. Araujo, A.G. Borrego, A.C. Cook, D. Flores, P.C. Hackley, J. Hower, M.L. Kern, K. Kommeren, J. Kus, M. Mastalerz, J.O. Mendonça, T.R. Menezes, J. Newman, P. Ranasinghe, I.V.A.F. Souza, I. Suarez-Ruiz, and Y. Ujjié, 2010, Effect of concentration of dispersed organic matter on optical maturity parameters: interlaboratory results of the organic matter concentration working group of the ICCP: *International Journal of Coal Geology*, v. 84, p. 154-165.

Merrill, G P., 1904, *The non-metallic minerals. Their occurrence and uses*: New York: John Wiley & Sons, London: Chapman & Hall, Limited, 387 p.

Milici R.C., R.T. Ryder, and F.T. Dulong, 2011, Appalachian Basin database for Devonian gas shales [abs]: AAPG 2011 Convention and Exhibition, April 10-13, 2011, Houston, Texas, Abstract 981838, p. 124, Search and Discovery Article #90124, Web accessed 13 April 2012. <http://www.searchanddiscovery.com/abstracts/html/2011/annual/abstracts/Milici.html>.

Nuccio, V.F., and J.R. Hatch, 1996, Vitrinite reflectance suppression in the New Albany Shale, Illinois Basin—Vitrinite reflectance and Rock-Eval data: U.S. Geological Survey Open-File Report 96-665, 37 p., <http://pubs.usgs.gov/of/1996/0665/report.pdf> (Accessed April 9, 2012).

Obermajer, M., M.G. Fowler, F. Goodarzi, and L.R. Snowdon, 1997, Organic petrography and organic geochemistry of Devonian black shales in southwestern Ontario, Canada: *Organic Geochemistry*, v. 26/3-4, p. 229-246.

Osborn, S.G., and J.C. McIntosh, 2010, Chemical and isotopic tracers of the contribution of microbial gas in Devonian organic-rich shales and reservoir sandstones, northern Appalachian Basin: *Applied Geochemistry*, v. 25, p. 456-471.

Price, L.C., and C.E. Barker, 1985, Suppression of vitrinite reflectance in amorphous rich kerogen – a major unrecognized problem: *Journal of Petroleum Geology*, v. 8, p. 59-84.

Repetski, J.E., R.T. Ryder, D.G. Weary, A.G. Harris, and M.H. Trippi, 2008, Thermal maturity patterns (CAI and %R<sub>o</sub>) in Upper Ordovician and Upper Devonian rocks of the Appalachian Basin: A major revision of USGS Map I-917-E using new subsurface collections: U.S. Geological Survey Scientific Investigations Map SIM-3006, 3 sheets, 1 pamphlet. Web accessed 17 April 2012. <http://pubs.usgs.gov/sim/3006/>.

Robert, P., 1988, *Organic metamorphism and geothermal history: microscopic study of organic matter and thermal evolution of sedimentary basins*: Elf Aquitaine, Dordrecht, 311 p.

Rowan, E.L., R.T. Ryder, J.E. Repetski, M.H. Trippi, and L.F. Ruppert, 2004, Initial results of a 2D burial/thermal history model, central

Appalachian Basin, Ohio and West Virginia: U.S. Geological Survey Open-File Report 2004-1445, 12 p., 15 figs. Web accessed 17 April 2012. <http://pubs.usgs.gov/of/2004/1445/>.

Rowan, E L., 2006, Burial and thermal history of the central Appalachian Basin, based on three 2-D models of Ohio, Pennsylvania, and West Virginia: U.S. Geological Survey Open-File Report 2006-1019, 35 p. Web accessed 17 April 2012. <http://pubs.usgs.gov/of/2006/1019/>.

Ruppert, L.F, J.C. Hower, R.T. Ryder, J.R. Levine, M.H. Trippi, and W.C. Grady, 2010, Geologic controls on thermal maturity patterns in Pennsylvanian coal-bearing rocks in the Appalachian Basin: International Journal of Coal Geology, v. 81, p. 169-181.

Ryder, R.T., 2008, Assessment of Appalachian Basin oil and gas resources: Utica-Lower Paleozoic Total Petroleum System: U.S. Geological Survey Open-File Report 2008-1287, 29 p.

Ryder, R.T., C.S. Swezey, R.D. Crangle, and M.T. Trippi, 2008, Geologic cross-section E-E' through the Appalachian Basin from the Findlay Arch, Wood County, Ohio, to the Valley and Ridge Province, Pendleton County, West Virginia: U.S. Geological Survey Scientific Investigations Map 2985, 2 sheets, 1 pamphlet. Web accessed 17 April 2012. <http://pubs.usgs.gov/sim/2985/>.

Simard, C., 1985, Grahamite and the Ritchie mine: Mountain State Geologist, v. 1985, p. 13-15.

Teichmüller, M., and K. Ottenjann, 1977, Art und diagenese von liptiniten und lipoiden stoffen in einem erdölmuttergestein aufgrund fluoreszenzmikroskopischer Untersuchungen: Erdöl und Kohle, Erdgas, Petrochemie, v. 30, p. 387-398.

Streib, D.L., 1981, Distribution of gas, organic carbon, and vitrinite reflectance in the eastern Devonian gas shales and their relationship to the geologic framework: U.S. Department of Energy, Morgantown Energy Technology Center, Report METC/08216-1276, 262 p.

Zielinski, R.E., and R.D. McIver, 1982, Resource and exploration assessment of the oil and gas potential in the Devonian gas shales of the Appalachian Basin: Mound Facility operated by Monsanto Research Corporation for the U.S. Department of Energy, contract No. DE-ACO4-76-DP00053, Report MLM-MU-82-61-0002 DOE/DP/0053-1125, 326 p., 2 appendices.

Transect A (main and ancillary data points)

Abbreviations used: A Abundant, C Common, Co Conodonts, Co<sub>A</sub> Conodonts (abundant), Co<sub>L</sub> Conodonts (local), L Local, L<sub>CD</sub> Local (from core description), Lg Linguloid, Lg<sub>C</sub> Linguloid (common), N none observed, NS, no sample, T Tasmanites, T<sub>A</sub> Tasmanites (abundant), T<sub>C</sub> Tasmanites (common), T<sub>L</sub> Tasmanites (local), Te Tentaculites, Te<sub>C</sub> Tentaculites (common), X present, X(A) present (abundant), X(C) present (common), X(L) present (local).

American Petroleum Institute number	Latitude (decimal degrees)	Longitude (decimal degrees)	Well on Transect	Lease name	County	State	Township or Quadrangle (7.5')	Sample No.	Formation	Interval sampled (ft)	Sample Type	Fossils	Bitumen
34-043-20005	41.39594118	-82.54485625	A <sub>1</sub>	N.Y., Chicago, & St. Louis Railroad (Core 734)	Erie	Ohio	Huron Twp.	A <sub>1</sub>	Huron Member of Ohio Shale	73-75	core	T <sub>C</sub>	N
34-093-21100	41.22613346	-82.02591146	A <sub>2</sub>	B & R McGuire (Core 2909) (OH-5)	Lorain	Ohio	Grafton Twp.	A <sub>2</sub>	Huron Member of Ohio Shale	1,072-1,073	core	T <sub>C</sub> , Lg	L <sub>CD</sub> , N
34-153-60416	41.01541419	-81.65529901	A <sub>3</sub>	Core 510	Summit	Ohio	Norton Twp.	A <sub>3a</sub>	Huron Member of Ohio Shale	1,880-1,886	core	T <sub>L</sub>	L
								A <sub>3b</sub>	Rhinestreet Shale	2,050-2,054	core	T <sub>L</sub> , Lg	L
								A <sub>3c</sub>	Marcellus Shale	2,176-2,180	core	Te, T <sub>L</sub> (dark)	N
34-155-21238	41.14683235	-80.91297921	A <sub>4</sub>	M & A Meleski (OH-7) (also Core 2962)	Trumbull	Ohio	Newton Twp.	A <sub>4a</sub>	Rhinestreet Shale	2,528	core	T <sub>L</sub>	L
								A <sub>4b</sub>	Marcellus Shale	2,697-2,698	core	T <sub>L</sub> (dark)	N
37-073-20022	41.09200528	-80.28192361	A <sub>C</sub>	No. 1 Sokevitz (PA-5)	Lawrence	Pa.	New Castle North Quad.	A <sub>Ca</sub>	Marcellus Shale	3,984	core	Co <sub>A</sub> , T <sub>L</sub> (dark), Lg	L
								A <sub>Cb</sub>	Marcellus Shale	4,124	core	NS	NS
37-121-22642	41.41419528	-79.8093475	A <sub>6</sub>	No. 348 Grant Fee	Venango	Pa.	Franklin Quad.	A <sub>6</sub>	Marcellus Shale	4,320-4,350	cuttings	NS	NS
37-053-20903	41.48463111	-79.29677583	A <sub>7</sub>	No. 1 Collins-Clinger	Forest	Pa.	Tylerville Quad.	A <sub>7</sub>	Marcellus Shale	4,970-5,020	cuttings	N	? (greasy appearance)
34-085-20017	41.75489757	-81.28214872	ALake	New York Central System (Core 855)	Lake	Ohio	Painesville Twp.	ALake <sub>a</sub>	Huron Member of Ohio Shale	841-843	core	T <sub>L</sub> , Co <sub>L</sub>	N
								ALake <sub>b</sub>	Rhinestreet Shale	952-954	core	T <sub>C</sub>	N (Sample looks bleached; recrystallized; silty)
								ALake <sub>c</sub>	Marcellus Shale	1,156-1,158	core	Lg <sub>C</sub> , Te <sub>C</sub> , T <sub>L</sub> , Co <sub>L</sub>	N
34-007-21087	41.94016595	-80.55170368	AAsh	Bessemer & Lake Erie Railroad Co. (OH-4) (Core 2839)	Ashtabula	Ohio	Conneaut Twp.	AAsh <sub>a</sub>	Rhinestreet Shale	1,172-1,173	core	T <sub>C</sub> (dark)	L <sub>CD</sub> , L
								AAsh <sub>b</sub>	Marcellus Shale	1,342-1,343	core	T <sub>L</sub>	L

Table 1. Data collected and analyzed on transect A (1 of 5).

Transect A (main and ancillary data points)								
American Petroleum Institute number	Dispersed macerals							Spectral Fluorescence, Mean $\lambda_{max}$
	Bituminite and (or) alginite (amorphous kerogen)	Telalginate	Vitrinite	Inertinite	Asphalt	Bitumen	Pyrobitumen	
34-043-20005	X (A) 	X (A) Tasmanites and Leosphaeridia(?) 	X 			X 		554
34-093-21100	X 	X (A) Leosphaeridia(?) 	X 	X		X 		531
34-153-60416	X 	X 	X 	X		X 		551
	X 	X 	X 			X 		555
	X 	X (brightly fluor. Leiosphaeridia(?)) 	X 	X (fusinite)	X	X (void filling) associated with carbonates 		610
34-155-21238	X (partially converted to bitumen network) 	X 	X 	X	X	X 		599 614
	X (converted to bitumen network) 	X (brightly fluor.) (macerated as well as leptodetrinite) 		X	X	X 	X	615
37-073-20022				X		X (A) bitumen network		
37-121-22642								
37-053-20903			X	X		X (A) bitumen network		
34-085-20017	X 	X (A) Tasmanites abn. 	X 	X				535
	X(A) 	X 	X 				Bitumen (0.81 Ro, others above and below 0.52)	583
		X (A) - lacks internal reflections and high relief / strong color 	X (c) 				X (local) 	581
34-007-21087	X (A) 	brightly fluor. X (A) 	X 	X (fusinite)		X 		567
	X (A) 	brightly fluor. X (A) 	X 	X (fusinite)				592

Table 1. Data collected and analyzed on transect A (2 of 5). Thumbnails are linked to full-size images in Part 2.

Transect A (main and ancillary data points)					
American Petroleum Institute number	Minerals				
	Pyrite	Carbonate	Quartz	Quartz / rutile	Clay-rich fragments
34-043-20005	X(A) framboids				
34-093-21100	X			X	
34-153-60416	X(A) framboids				
	X (A) framboids	X (A) rhomb			
34-155-21238	X (framboids)	X (nodules and rhombs)			
37-073-20022	X	X (dolo.)			
37-121-22642					
37-053-20903	X (A) framboids				
34-085-20017	X (A) framboids			X	
	X (A) framboids commonly associated with telalginite	X calcite rhombs	X		
34-007-21087	X (framboids) associated with telalginite	X rhombs			
	X (A) framboids				

Table 1. Data collected and analyzed on transect A (3 of 5).

Transect A (main and ancillary data points)									
American Petroleum Institute number	Total Organic Carbon (in wt. %)		Rock Eval						
	TOC	TOC Streib (1981)	S <sub>1</sub>	S <sub>2</sub>	S <sub>3</sub>	HI	OI	T <sub>max</sub>	PI
34-043-20005	5,8		1,44	25,85	0,4	446	7	429	0,05
34-093-21100	5,66		2,74	24,14	0,28	427	5	434	0,1
34-153-60416	9,21		4,76	39,42	0,46	428	5	440	0,11
	6,95		2,35	26,96	0,43	388	6	437	0,08
	6,33		1,49	25,18	0,34	398	5	438	0,06
34-155-21238	8,44		5,67	37,02	0,18	439	2	440	0,13
	5		4,6	18,16	0,38	363	8	444	0,2
37-073-20022	12,25		6,26	24,06	1,41	196	12	433	0,21
	4,54		3,28	6,94	0,48	153	11	440	0,32
37-121-22642	4,6		3,78	7,48	0,43	163	9	436	0,34
37-053-20903	6,1		2,53	3,19	0,62	52	10	454	0,44
34-085-20017	6,67		4,61	31,7	0,53	475	8	437	0,13
	2,11		0,57	4,78	0,3	227	14	436	0,11
	6,19		4,53	27,2	0,5	439	8	438	0,14
34-007-21087	6,63		2,96	28,76	0,29	434	4	442	0,09
	7,89		2,98	28,03	0,35	358	4	440	0,1

Table 1. Data collected and analyzed on transect A (4 of 5).

Transect A (main and ancillary data points)									
American Petroleum Institute number	Vitrinite Reflectance						Gas chromatography of bitumen extract		
	%Ro <sub>mean</sub> Humble	%Ro <sub>mean</sub> Humble (corrected)	%Ro <sub>mean</sub> Hackley	%Ro <sub>mean</sub> Streib (1981)	%Ro <sub>mean</sub> Zielinski and McIver (1982)	%Ro <sub>mean</sub> ExLog	Gas chromatography image	GC Code	Pristane / Phytane
34-043-20005	0.45	0.69							2.26
34-093-21100	0.36	0.49			0.56				0.96
34-153-60416	0.47	0.72	0.5						2.21
	0.47	0.62	0.48						1.99
	0.48	0.67	0.49						1.41
34-155-21238	0.42	0.61	0.46		0.56				1.87
	0.42	0.54	0.53		0.62				1.43
37-073-20022			0.96		1				1.30
	0.41	0.43 (corrected by authors using Lo, 1993)			1				
37-121-22642	0.47	0.59 (corrected by authors using Lo, 1993)							
37-053-20903	0.94								ND
34-085-20017	0.38	0.56	0.5						2.05
	0.42	0.48	0.81						2.17
	0.46	0.68	0.52						1.18
34-007-21087	0.38	0.56	0.48	0.40-0.54 med. = 0.44 n=23	0.44				1.90
	0.37	0.45	0.5	0.44-0.59 med. = 0.52 n=5	0.46				1.49

Table 1. Data collected and analyzed on transect A (5 of 5). Thumbnails are linked to full-size images in Part 2.

Transect B (main and ancillary data points)

Abbreviations used: A Abundant, C Common, Co Conodonts, Co <sub>2</sub> Conodonts (abundant), Co <sub>1</sub> Conodonts (local), L Local, L <sub>CD</sub> Local (from core description), Lg Linguloid, Lg <sub>2</sub> Linguloid (common), N none observed, NS, no sample, T Tasmanites, T <sub>A</sub> Tasmanites (abundant), T <sub>C</sub> Tasmanites (common), T <sub>L</sub> Tasmanites (local), Te Tentaculites, Te <sub>C</sub> Tentaculites (common), X present, X(A) present (abundant), X(C) present (common), X(L) present (local).													
American Petroleum Institute number	Latitude (decimal degrees)	Longitude (decimal degrees)	Well on Transect	Lease name	County	State	Township or Quadrangle (7.5')	Sample No.	Formation	Interval sampled (ft)	Sample Type	Fossils	Bitumen
34-117-60037	40.4774015	-82.78926321	B <sub>1</sub>	Core 2770	Morrow	Ohio	Harmony Twp.	B <sub>1</sub>	Huron Member of Ohio Shale	708-713	core	T <sub>A</sub>	N
34-083-22599	40.3977816	-82.50287591	B <sub>2</sub>	L. Beckhoit (OH-3) (Core 2900)	Knox	Ohio	Clinton Twp.	B <sub>2a</sub>	Huron Member of Ohio Shale	1,100-1,101	core	T <sub>A</sub>	N
								B <sub>2b</sub>	Rhinestreet Shale	1,188-1,189	core		
34-119-21617	40.01455938	-81.86942905	B <sub>3</sub>	W & D Winegardner	Muskingum	Ohio	Salem Twp.	B <sub>3</sub>	Huron Member of Ohio Shale	2,400-2,532	cuttings	T <sub>A</sub>	N
34-121-22255	39.71358062	-81.46210232	B <sub>4</sub>	H & M Shockling (OH-8) (Core 2936)	Noble	Ohio	Enoch Twp.	B <sub>4a</sub>	Huron Member of Ohio Shale	3,462-3,463	core	T <sub>C</sub> (dark)	N
								B <sub>4b</sub>	Rhinestreet Shale	3,999-4,000	core	T <sub>L</sub> (dark)	
								B <sub>4c</sub>	Marcellus Shale	4,094.8-4,095.4	core	T <sub>L</sub> (dark)	C
								B <sub>4d</sub>	Marcellus Shale	4,097.8-4,097.9	core	T <sub>L</sub> (dark)	C
34-013-20277	39.97860656	-80.84439782	B <sub>5</sub>	R. L. Brown (Core 2842)	Beimont	Ohio	Mead Twp.	B <sub>5</sub>	Marcellus Shale	5,574-5,577	core	Co <sub>1</sub> , T <sub>L</sub> (dark)	C
47-103-00645	39.67694	-80.82389	B <sub>6</sub>	Emch & Pyles No. 1 (WV-7)	Wetzel	W. Va.	New Martinsville Quad.	B <sub>6a</sub>	Rhinestreet Shale	6,246,30	core	T <sub>L</sub> (dark/faint)	C
								B <sub>6b</sub>	Marcellus Shale	6,599 and 6,618	core		
37-059-20038	39.86056556	-80.14601583	B <sub>7</sub>	No. 1 Gordon	Greene	Pa.	Oak Forest Quad.	B <sub>7</sub>	Marcellus Shale	7,860-7,960	cuttings	T <sub>L</sub> (amber)	
47-077-00086	39.466669	-79.870278	B <sub>8</sub>	No. A-1 H.G. Walls	Preston	W. Va.	Newburg Quad.	B <sub>8</sub>	Marcellus Shale	7,185-7,190	cuttings	N	

Table 2. Data collected and analyzed on transect B (1 of 5).

Transect B (main and ancillary data points)								
American Petroleum Institute number	Dispersed macerals							
	Bituminite and (or) alginite (amorphous kerogen)	Telalginite	Vitrinite	Inertinite	Asphalt	Bitumen	Pyrobitumen	Spectral fluorescence, mean $\lambda_{max}$
34-117-80037	X 	X 	X (A) 	X		X (local) 		517
34-083-22599	X with scattered telalginite 	X 	X 	X				519
34-119-21617		X 	X 	X 		X		554
34-121-22255	X  X 	X (L) weakly fluor. 	X   X slightly lower %Ro than pyrobitumen	X   X (fusinite)  X (fusinite)	X asphalt (L) 	X (anastomosing)  X  X	X?  X?  X dead oil (more abn. pyrobitumen than in Huron / Rhinestreet)  X pyrobitumen (impsonite) and asphalt (multiple generations), bituminous groundmass 	726  613  685  704
34-013-20277				X (fusinite)		X	X? (some pyrobitumen) anastomosing bitumen 	702
47-103-00845			X (scattered)	X (fusinite)			X? 	
37-059-20038			X 	X (fusinite)			X 	
47-077-00086			X some may be pyrobitumen	X (fusinite)			X (A) 	

Table 2. Data collected and analyzed on transect B (2 of 5). Thumbnails are linked to full-size images in Part 2.

Transect B (main and ancillary data points)					
American Petroleum Institute number	Minerals				
	Pyrite	Carbonate	Quartz	Quartz / rutile	Clay-rich fragments
34-117-60037	X (A)	X			
34-083-22599					
34-119-21617					
34-121-22255	X (A) in quartz-rich fragments	X	X (quartz-rich fragments)		X
	X pyrite-rich shale	X	X (quartz-rich fragments)	X	X
		X (rhombs)			
	X (C) framboids	X (rhombs)			
34-013-20277	X (A)				
47-103-00645	X (A) (framboids)				
37-059-20038					
47-077-00086	X (A) (framboids) 	X (authigenic)			

Table 2. Data collected and analyzed on transect B (3 of 5). Thumbnail is linked to full-size images in Part 2.

Transect B (main and ancillary data points)									
American Petroleum Institute number	Total Organic Carbon (in wt. %)		Rock Eval						
	TOC	TOC Streib (1981)	S <sub>1</sub>	S <sub>2</sub>	S <sub>3</sub>	HI	OI	T <sub>max</sub>	PI
34-117-60037	9,92		4,41	55,69	0,14	561	4	428	0,07
34-083-22599	7,2		4,74	39,13	0,25	543	3	439	0,11
34-119-21617	4,02		2,18	18,4	0,43	458	11	438	0,11
34-121-22255	7,03		4,5	17,52	0,14	252	2	449	0,2
	2,09		2,08	1,8	0,13	86	6	446	0,54
	4,40		2,74	10,95	0,22	249	5	442	0,20
	3,62		2,81	8,94	0,20	247	6	441	0,24
34-013-20277	5,97		3,58	3,62	0,22	61	4	443	0,50
47-103-00645	1,15	0.79 med; n=20	0,58	0,45	0,41	39	36	441	0,56
37-059-20038	5,92		1,15	3,07	0,56	52	9	406	0,27
47-077-00086	1,43		1,59	2,14	0,4	150	28	384	0,43

Table 2. Data collected and analyzed on transect B (4 of 5).

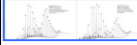
Transect B (main and ancillary data points)									
American Petroleum Institute number	Vitrinite Reflectance						Gas chromatography of bitumen extract		
	%Ro <sub>max</sub> Humble	%Ro <sub>max</sub> Humble (corrected)	%Ro <sub>max</sub> Hackley	%Ro <sub>max</sub> Streib (1981)	%Ro <sub>max</sub> Zielinski and McIver (1982)	%Ro <sub>max</sub> ExLog	Gas chromatography image	GC Code	Pristane/ Phytane
34-117-60037	0.43	0.73							1.90
34-083-22599	0.44	0.75	0.45	0.56 med. n=7	0.55				1.83
34-119-21617	0.38	0.51							
34-119-21617	0.43	0.66							1.83
34-121-22255	0.73	0.83	0.93			0.82			1.98
	1.01		0.99		1				1.54
			0.96		0.75				1.54
			0.93						1.54
34-013-20277	1.04		1.16						1.97
47-103-00645			1.56	1.58 med. n=18	1.62				
				1.71 n=2	1.76				
37-059-20038	1.44								1.51, 1.63
47-077-00086	1.6		2.03						1.50

Table 2. Data collected and analyzed on transect B (5 of 5). Thumbnails are linked to full-size images in Part 2.

Transect C (main and ancillary data points)

Abbreviations used: A Abundant, C Common, Co Conodonts, Co<sub>A</sub> Conodonts (abundant), Co<sub>L</sub> Conodonts (local), L Local, L<sub>CD</sub> Local (from core description), Lg Linguloid, Lg<sub>C</sub> Linguloid (common), N none observed, NS, no sample, T Tasmanites, T<sub>A</sub> Tasmanites (abundant), T<sub>C</sub> Tasmanites (common), T<sub>L</sub> Tasmanites (local), Te Tentaculites, Te<sub>C</sub> Tentaculites (common), X present, X(A) present (abundant), X(C) present (common), X(L) present (local).

American Petroleum Institute number	Latitude (decimal degrees)	Longitude (decimal degrees)	Well on Transect	Lease name	County	State	Township or Quadrangle (7.5')	Sample No.	Formation	Interval sampled (ft)	Sample Type	Fossils	Bitumen
34-049-60004	39,99690459	-82,80555431	C <sub>1</sub>	Core 859	Franklin	Ohio	Jefferson Twp.	C <sub>1</sub>	Huron Member of Ohio Shale	636-638	core	T <sub>A</sub>	N
34-045-20234	39,71695374	-82,38044488	C <sub>2</sub>	Merckle	Fairfield	Ohio	Rush Creek Twp.	C <sub>2</sub>	Huron Member of Ohio Shale	1,536-1,640	cuttings	T <sub>A</sub>	N
34-073-20497	39,44455447	-82,29964201	C <sub>3</sub>	Kappel	Hocking	Ohio	Starr Twp.	C <sub>3</sub>	Huron Member of Ohio Shale	1,995-2,070	cuttings	T <sub>A</sub>	N
34-105-22058	39,09108542	-81,86300335	C <sub>4</sub>	Newell (Core 2921) (OH-9)	Meigs	Ohio	Chester Twp.	C <sub>4</sub>	Huron Member of Ohio Shale	3,300-3,301	core	T <sub>A</sub> (dark), Co <sub>L</sub>	L
47-035-01371	38,873355	-81,848246	C <sub>5</sub>	No. 120401 W.L. Pinnell (WV-2)	Jackson	W. Va.	Cottageville Quad.	C <sub>5</sub>	Huron Member of Ohio Shale	3 564	core	T <sub>A</sub> (dark), Co <sub>L</sub>	L
47-035-00615	38,805835	-81,79583	C <sub>6</sub>	No. 1 Nellie Sayre King	Jackson	W. Va.	Cottageville Quad.	C <sub>6</sub>	Rhinestreet Shale	4,402-4,596	cuttings	T <sub>A</sub> (dark), Co <sub>L</sub>	L
47-039-00205	38,427776	-81,557778	C <sub>7</sub>	No. 1 Robertson (GW-346)	Kanawha	W. Va.	Big Chimney Quad.	C <sub>7</sub>	Rhinestreet Shale	4,605-4,896	cuttings	T <sub>A</sub> ? (dark with faint outline)	L
47-087-00019	38,781388	-81,503891	C <sub>8</sub>	Heinzman (4053)	Roane	W. Va.	Gay Quad.	C <sub>8</sub>	Rhinestreet Shale	4,840-5,200	cuttings	T <sub>L</sub>	N

Table 3. Data collected and analyzed on transect C (1of 5).

Transect C (main and ancillary data points)

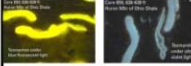
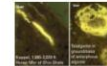
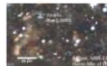
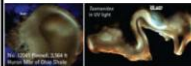
American Petroleum Institute number	Dispersed macerals							Spectral fluorescence; mean $\lambda_{max}$
	Bituminite and (or) Alginite (amorphous kerogen)	Telaiginite	Vitrinite	Inertinite	Asphalt	Bitumen	Pyrobitumen	
34-049-60004	X (A) with scattered telaiginite 	X(A) brightly greenish fluor., numerous <u>Tasmanites</u> 	X 	X (fusinite) 				522
34-045-20234	X (A) 	X 	X 	X 		X 		543
34-073-20497	X with scattered telaiginite 	X 	X 	X 		X 		535
34-105-22058		X (A) 	X 	X 		X 		611
47-035-01371		X (A) 	X 	X 		X 		612
47-035-00615								
47-039-00205								
47-087-00019								

Table 3. Data collected and analyzed on transect C (2 of 5). Thumbnails are linked to full-size images in Part 2.

Transect C (main and ancilliary data points)

American Petroleum Institute number	Minerals				
	Pyrite	Carbonate	Quartz	Quartz / rutile	Clay-rich fragments
34-049-60004					
34-045-20234	X	X (rhombs)		X	
34-073-20497	X (framboids)				
34-105-22058	X(A) (framboids)			X	
47-035-01371					
47-035-00615					
47-039-00205					
47-087-00019					

Table 3. Data collected and analyzed on transect C (3 of 5).

Transect C (main and ancillary data points)

American Petroleum Institute number	Total Organic Carbon (in wt. %)		Rock Eval						
	TOC	TOC Streib (1981)	S <sub>1</sub>	S <sub>2</sub>	S <sub>3</sub>	HI	OI	T <sub>max</sub>	PI
34-049-60004	7,32		2,04	36,31	0,42	496	6	433	0,05
34-045-20234	5,95		3,03	29,01	0,57	488	10	432	0,09
34-073-20497	5,22		2,51	25,91	0,49	496	9	434	0,09
34-105-22058	5,52		4,34	21,68	0,22	392	4	448	0,17
47-035-01371	4,99		2,91	24,38	1,42	488	28	441	0,11
47-035-00615	2,12		0,77	3,21	0,37	151	17	440	0,19
47-039-00205	1,89		1,2	1,4	0,68	74	36	448	0,46
47-087-00019	1,22		1,23	2	0,38	164	31	396	0,38

Table 3. Data collected and analyzed on transect C (4 of 5).

Transect C (main and ancillary data points)

American Petroleum Institute number	Vitrinite Reflectance						Gas chromatography of bitumen extract		
	%Ro <sub>mean</sub> Humble	%Ro <sub>mean</sub> Humble (corrected)	%Ro <sub>mean</sub> Hackley	%Ro <sub>mean</sub> Streib (1981)	%Ro <sub>mean</sub> Zielinski and McIver (1982)	%Ro <sub>mean</sub> ExLog	Gas chromatography image	GC Code	Pristane / Phytane
34-049-60004	0,44	0,73	0,53						1,92
34-045-20234	0,44	0,71	0,47						1,61
34-073-20497	0,39	0,62	0,45						2,00
34-105-22058	0,48	0,67	0,53		Mean 0,5	0,59			1,83
47-035-01371			0,54						2,27
47-035-00615	0,72								
47-039-00205	0,85								
47-087-00019	1,02								

Table 3. Data collected and analyzed on transect C (5 of 5). Thumbnails are linked to full-size images in Part 2.

Transect D (main and ancilliary data points)

American Petroleum Institute number	Latitude (decimal degrees)	Longitude (decimal degrees)	Well on Transect	Lease name	County	State	Township or Quadrangle (7.5')	Sample No.	Formation	Interval sampled (ft)	Sample Type	Fossils	Bitumen
34-145-60142	38,86479477	-83,20466644	D <sub>1</sub>	Core 2814	Scioto	Ohio	Brush Creek Twp.	D <sub>1</sub>	Huron Member of Ohio Shale	480-481	core	T <sub>A</sub>	N
16-043-16235	39,293272	-83,111354	D <sub>2</sub>	No. 11-1 Warnie Stapleton	Carter	Ky.	Grahn Quad.	D <sub>2</sub>	Huron Member of Ohio Shale	1,220-1,260	cuttings	T <sub>L</sub>	N
16-063-26619	38,120524	-82,955943	D <sub>3</sub>	No. 3 I.R. Ison (Stephens Unit)	Elliott	Ky.	Mazie Quad.	D <sub>3</sub>	Huron Member of Ohio Shale	1,520-1,570	cuttings	T <sub>C</sub>	N
16-115-63403	37,859252	-82,984129	D <sub>4</sub>	No. 4 Conley	Johnson	Ky.	Oil Springs Quad.	D <sub>4</sub>	Huron Member of Ohio Shale	1,290-1,360	cuttings	T <sub>C</sub> (dark)	N
47-043-01656	38,096671	-82,240838	D <sub>5</sub>	Columbia/McCoy (20402) (WV-4)	Lincoln	W.Va.	Ranger Quad.	D <sub>5</sub>	Huron Member of Ohio Shale	3 542	core	T <sub>A</sub> (dark)	L
16-145-82020	37,52161	-82,277058	D <sub>6</sub>	No. 69 Ford Motor Co.	Pike	Ky.	Belfry Quad.	D <sub>6</sub>	Huron Member of Ohio Shale	4 387,5	core	T <sub>C</sub> (dark)	L
45-027-20147	37,24702238	-82,18590051	D <sub>7</sub>	No. 9781 Pittston	Buchanan	Va.	Prater Quad.	D <sub>7</sub>	Huron Member of Ohio Shale	5,320-5,340	cuttings	N	N

Table 4. Data collected and analyzed on transect D (1 of 5).

Transect D (main and ancillary data points)

American Petroleum Institute number	Dispersed macerals							Spectral fluorescence; mean $\lambda_{max}$
	Bituminite and (or) alginite (amorphous kerogen)	Telalginite	Vitrinite	Inertinite	Asphalt	Bitumen	Pyrobitumen	
34-145-60142	X 	X 	X (A) 	X 		X 		538
16-043-16235	X 	X 	X 	X 		X 		559
16-063-26619	X (A) 	X (A) 	X? 	X (fusain) 		X 		562
16-115-63403		X 		X 		X (A) 		552
47-043-01656		X 				X (A) 		661
16-145-82020				X (fusain) 		X 		
45-027-20147				X (fusain) 		X 		

Table 4. Data collected and analyzed on transect D (2 of 5). Thumbnails are linked to full-size images in Part 2.

Transect D (main and ancillary data points)

American Petroleum Institute number	Minerals				
	Pyrite	Carbonate	Quartz	Quartz / rutile	Clay-rich fragments
34-145-60142	X (A)			X	
16-043-16235	X (A)				
16-063-26619					
16-115-63403					
47-043-01656					
16-145-82020					
45-027-20147				X	



Table 4. Data collected and analyzed on transect D (3 of 5). Thumbnail is linked to full-size images in Part 2.

Transect D (main and ancilliary data points)

American Petroleum Institute number	Total Organic Carbon (in wt. %)		Rock Eval						
	TOC	TOC Streib (1981)	S <sub>1</sub>	S <sub>2</sub>	S <sub>3</sub>	HI	OI	T <sub>max</sub>	PI
34-145-60142	9,57		4,03	51,04	0,65	533	7	433	0,07
16-043-16235	6,76		2,46	27,68	0,51	409	8	429	0,08
16-063-26619	9,05		3,4	37,38	1,1	413	13	434	0,08
16-115-63403	6,43		2,02	27,09	0,84	421	13	433	0,07
47-043-01656	6,36		4,2	22,24	0,4	350	6	448	0,16
16-145-82020	6,01		1,78	3,72	0,25	62	4	463	0,32
45-027-20147	2,15		4,01	4,85	0,67	226	31	409	0,45

Table 4. Data collected and analyzed on transect D (4 of 5).

Transect D (main and ancillary data points)

American Petroleum Institute number	Vitrinite Reflectance						Gas chromatography of bitumen extract		
	%Ro <sub>mean</sub> Humble	%Ro <sub>mean</sub> Humble (corrected)	%Ro <sub>mean</sub> Hackley	%Ro <sub>mean</sub> Streib (1981)	%Ro <sub>mean</sub> Zielinski and McIver (1982)	%Ro <sub>mean</sub> ExLog	Gas chromatography image	GC Code	Pristane/Phytane
34-145-60142	0,33	0,53	0,53						1,69
16-043-16235	0,59	0.78 (corrected by authors using Lo, 1993)	0,66						1,44
16-063-26619	0,58	0.78 (corrected by authors using Lo, 1993)	0,5						1,72
16-115-63403	0,45	0.62 (corrected by authors using Lo, 1993)	0,61						1,68
47-043-01656	0,51	0.62 (corrected by authors using Lo, 1993)	0,66						1,83
16-145-82020	0,75		1,42						1,18
45-027-20147	1,76		1,85						

Table 4. Data collected and analyzed on transect D (5 of 5). Thumbnails are linked to full-size images in Part 2.